Mahidol University Center for Scientific Computing

2013 Annual Report

C. Boonyasiriwat, N. Boonyasiriwat, A. Nakpathom,
and J. Sinsawasmongkol

May 9, 2014

Contents

Part I Signal Processing

A new method based on seismic interferometry for reducing surface-wave noise in seismic data
Chaiwoot Boonyasiriwat and Jaroon Sinsawasmongkol 1

Surface-wave noise prediction using elastic waveform modeling
Jaroon Sinsawasmongkol and Chaiwoot Boonyasiriwat 5

A Fortran 90 implementation of matching filter
Chaiwoot Boonyasiriwat 15

Part II Migration and Inversion

Kirchhoff full-waveform inversion: A synthetic study
Chaiwoot Boonyasiriwat 19

Visco-acoustic full-waveform inversion in the frequency-space domain
Apirujee Nakpathom and Chaiwoot Boonyasiriwat 23

Kirchhoff prestack depth migration of 2D Isan land data
Chaiwoot Boonyasiriwat 33

Part III Software Development

MMI: A software package for seismic modeling, migration, and inversion
Chaiwoot Boonyasiriwat 37

JIMMI: Java Interface to MMI
Numchoke Boonyasiriwat and Chaiwoot Boonyasiriwat 41

MCSC ANNUAL REPORT 2013

This report summarizes the annual 2013 research accomplishments of the researchers of the Mahidol University Center for Scientific Computing (MCSC). MCSC is mainly supported by the PTT Exploration and Production Plc. through the funded research project titled "Development of Geophysical Methods for Petroleum Exploration". This annual report is comprised of individual report of each research project conducted at MCSC.

Thanks for your support,

Chaiwoot Boonyasiriwat and colleagues
Mahidol University Center for Scientific Computing
Department of Physics, Faculty of Science, Mahidol University
272 Rama VI Road, Ratchathewi, Bangkok 10400, THAILAND
Phone: 66-2-201-5771, 66-2-201-5734
Fax: 66-2-354-7159
Email: chaiwoot@gmail.com
Website: http://mcsc.sc.mahidol.ac.th

Part I

Signal Processing

A new method based on seismic interferometry for reducing surface-wave noise in seismic data

Chaiwoot Boonyasiriwat and Jaroon Sinsawasmongkol

ABSTRACT

A new method based on seismic interferometry is presented for reducing surface-wave noise in land seismic data. This method is much simpler than the conventional interferometric method previously proposed. The efficiency and effectiveness of our method is shown by the application to land data acquired in a north-east area of Thailand.

INTRODUCTION

Surface waves are evanescent wave that propagates along a free surface of a medium. In the case of seismic wave, two types of surface waves, Rayleigh and Love waves, occur due to the interference of body P-waves and S-waves. Rayleigh wave is generated by the interference of P-wave and SV-wave while Love wave is generated by the interference of P-wave and SH-wave. Rayleigh wave or usually called groundroll is the surface wave that is recorded by geophones recording vertical ground motion. In seismic exploration, the vertical-ground-motion data or seismograms (vertical particle displacement, velocity, or acceleration) are usually used in seismic reflection data processing to obtain an image of the Earth's subsurface structures. In this situation, primary reflections are normally the signal while the other events including direct waves, refractions, multiple reflections, and surface waves are considered as noise.

Land seismic data are usually corrupted with strong surface-wave noise which, therefore, is the main noise that must be removed to enhance the signal-to-noise ratio of seismic reflection data and to prevent any artifacts due to the noise in the seismic section obtained after data processing. Many methods to reduce the surface-wave noise have been proposed in the past decades. Among these methods seismic interferometry (Halliday et al., 2007, 2010; Xue et al., 2009; Xue, 2010) is one of the efficient methods that can be applied even when there is an aliasing issue of surface-wave events in the data. The key idea of the seismic interferometry method for reducing surface-wave noise is to first create a prediction of the noise by cross-correlating data traces, and then to adaptively subtract the predicted noise from the data. The signal-to-noise ratio of the prediction is improved by stacking predicted traces from many common shot gathers from various source positions. This simple idea can become quite complicated to implement into a compute program that can be universally applied to any seismic data set.

In this work, we propose a new method based on seismic interferometry that is much simpler than the previously proposed method. The key improvement of our method is that the prediction of surface-wave noise in a common shot gather (CSG) can be obtained by processing the same CSG using cross-correlation and convolution of data traces. Therefore, the proposed filtering method can easily be applied to any data set. The efficiency and effectiveness of the method is shown in the application to a land data set acquired in a north-east area of Thailand.

In the next section, we briefly describe the conventional seismic interferometry method for predicting surface-wave noise. Then, the new method is presented in the consecutive section. Numerical results are then shown with a discussion followed by a conclusion.

CONVENTIONAL SEISMIC INTERFEROMETRY METHOD FOR PREDICTING SURFACE-WAVE NOISE

Consider a surface wave propagating from a source at s_1 to receivers at g_1 and g_2 as shown in Figure 1. The time-domain surface-wave event recorded at g_1 and g_2 are denoted as $d(g_1|s_1)$ and $d(g_2|s_1)$, respectively, where their frequency-domain counterparts are denoted as $D(g_1|s_1)$ and $D(g_2|s_1)$. Using the high-frequency approximation and ignoring amplitude factor, the surface-wave data in

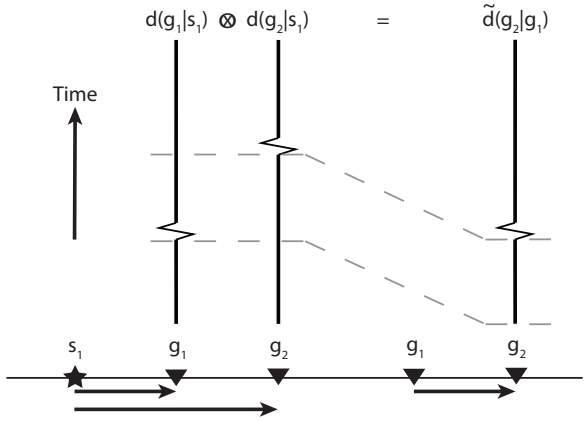

Figure 1: The key diagram that demonstrated how seismic interferometry (cross-correlating two data traces) can be used to predict surface wave propagating from position g_1 to g_2. (For more details, please see the text.)

the frequency domain can be represented by

$$D(g_1|s_1) = e^{i\omega\tau_{s_1g_1}}, \tag{1}$$

and

$$D(g_2|s_1) = e^{i\omega\tau_{s_1g_2}}, \tag{2}$$

where $\tau_{s_1g_1}$ and $\tau_{s_1g_2}$ are the traveltimes of surface wave propagating from s_1 to g_1 and g_2, respectively.

Recalling the cross-correlation theorem

$$f \otimes g = \mathcal{F}^{-1}(\mathcal{F}(f)^*\mathcal{F}(g)) \tag{3}$$

where f and g are two functions, $\mathcal{F}$ and $\mathcal{F}^{-1}$ denote the direct and invert Fourier transform operators, respectively, and $*$ denotes the complex conjugate. Applying the cross-correlation theorem to the surface wave data $d(g_1|s_1)$ and $d(g_2|s_1)$ yields

$$\begin{aligned} d(g_1|s_1) \otimes d(g_2|s_1) &= \mathcal{F}^{-1}\left(\mathcal{F}(d(g_1|s_1))^*\mathcal{F}(d(g_2|s_1))\right) \\ &= \mathcal{F}^{-1}\left(D(g_1|s_1)^*D(g_2|s_1)\right) \\ &= \mathcal{F}^{-1}\left((e^{i\omega\tau_{s_1g_1}})^*e^{i\omega\tau_{s_1g_2}}\right) \\ &= \mathcal{F}^{-1}\left(e^{i\omega(\tau_{s_1g_2}-\tau_{s_1g_1})}\right) \end{aligned} \tag{4}$$

According to equation 4, cross-correlating the two data traces cancels the phase of the common raypath of surface wave and yields a virtual data trace of surface wave propagating from g_1 to g_2 denoted by $\tilde{d}(g_2|g_1)$ as shown in Figure 1.

Since the data traces $d(g_1|s_1)$ and $d(g_2|s_1$ also contain other seismic events such as reflections, the predicted surface-wave trace obtained always contains some noise. The conventional interferometric prediction method improves the signal-to-noise ratio (S/N) of the prediction by stacking virtual traces obtained from many common shot gathers containing geophones at the same position g_1 and g_2. Suppose there are n of these CSGs with shot positions $s_1, s_2, ..., s_n$ as shown in Figure 2. The S/N of the

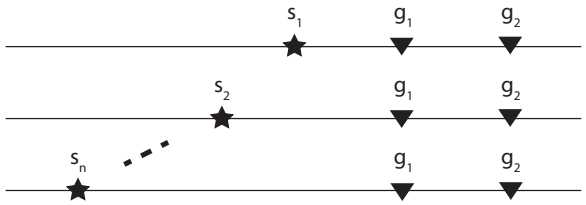

Figure 2: The diagram showing n shot positions, $s_1, s_2, ..., s_n$, with common geophones at g_1 and g_2.

surface-wave prediction can be increased by a factor of $\sqrt{n}$ by averaging these virtual traces:

$$\tilde{d}(g_2|g_1) = \frac{1}{n}\sum_{i=1}^{n} d(g_1|s_i) \otimes d(g_2|s_i). \tag{5}$$

Once the surface-wave prediction is obtained, an adaptive subtraction is applied to reduce surface-wave noise from the original data. The reason that we cannot simply subtract the prediction directly from the data is that the phase and amplitude of the surface-wave prediction are usually incorrect compared to those of the actual surface-wave noise. For more rigorous description of the method, the reader is recommended to see the work of Xue et al. (2009).

The principle of this method is quite simple but some issues arise when we want to implement the method into an efficient computer program that can be applied to predict surface waves in all CSGs of any data set. These issues are as follows.

- To predict surface waves propagating from position g_i to g_j in a CSG, the computer program needs to search for CSGs that contain geophones at g_i and g_j, and perform cross-correlation and trace averaging to obtain one predicted trace. Consequently, to obtain a predicted virtual gather, the computer program needs to perform a large amount of data searching which could cause the program to be inefficient.
- The computer program may take a long time to process the data if the entire data set cannot be loaded into the computer memory since the program needs to load CSG data several times. This is due to the fact that computer time for loading data from storage devices such hard disk is several orders of magnitude slower than performing calculation.

These problems can be overcome if the process of predicting surface waves in a CSG only requires data within that CSG. This is the key improvement of the new method proposed in the next section.

A NEW SEISMIC INTERFEROMETRY METHOD FOR PREDICTING SURFACE-WAVE NOISE

In this section, we describe the new method based on seismic interferometry for predicting surface-wave noise in

seismic land data. To solve the issues of the conventional method, we use both cross-correlation and convolution of data traces as shown in Figure 3. In this method, we first choose a small-offset reference trace $d(g_1|s)$ (g_1 is close to the source position s). The second trace must be recorded by geophone at g_2 whose offset is larger than g_1. Then, the two traces are cross-correlated to obtain a virtual trace $\tilde{d}(g_2|g_1)$. This is the first step of the method which is the same as the conventional method. The second step is to apply convolution of the virtual trace and the reference trace to obtain a surface-wave prediction $\tilde{d}(g_2|s)$. This can be summarized as

$$\tilde{d}(g_2|g_1) = d(g_1|s) * [d(g_1|s) \otimes d(g_2|s)]. \quad (6)$$

The idea of using both cross-correlation and convolution is borrowed from the refraction interferometry work of (Mallinson et al., 2011; Bharadwaj et al., 2012).

To increase the S/N of the prediction, the two-step process (equation 6) is iteratively applied to the virtual trace as shown in the pseudocode:

```
p(g2,s) = d(g2,s)
for i from 1 to n
  p(g2,s) = d(g1,s) * [ d(g1,s) x p(g2,s) ]
end
```

Here $\times$ denotes the cross-correlation operator and `p(g2,s)` is the final prediction after n iterations. The geophone position g_2 is then varied to obtain the prediction for the rest of geophones which are on the same side with respect to the source position as the reference geophone g_1. The same procedure is then repeated for geophones on the other side to obtain a complete prediction for the CSG of interest. It is worth noting that we do not obtain surface-wave predictions at the two reference traces and possibly at a few geophone positions with smaller offset than the reference geophones.

Once the prediction is obtained for a CSG, the adaptive subtraction is then applied to reduce surface-wave noise from the CSG. This process is the same as the conventional method.

FIELD DATA RESULTS

To evaluate the effectiveness of the proposed seismic interferometry method, we applied the proposed method and FK filtering to the land data from PTTEP. The filtering result is shown in Figure 4. Figures 4a and 4b show the filtering result from FK filtering for common shot gather number 10 (CSG10). The result shows that seismic interferometry is more effective in reducing surface-wave noise in the data than FK filtering. In this case, FK filtering is not so effective due to the aliasing of surface-wave events. As expected, seismic interferometry filtering is immune to the aliasing problem. However, there is still residual surface-wave noise left in the filtering result. We remove the residual noise using FK filtering (Figure 4c). Although we did not show the filtering result from the conventional

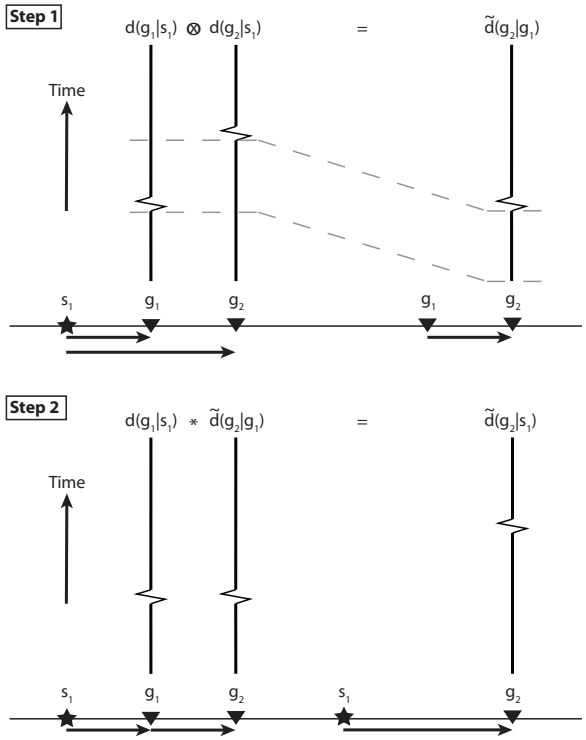

Figure 3: The key diagram that demonstrated how the new seismic interferometry method can predict surface wave propagating from position s to g_2 using both cross-correlation ($\otimes$) and convolution ($*$).

seismic interferometry filtering, we expect it to be as effective as the new method. However, we need to compare the two methods in the future. In addition, we need to apply the proposed method to more data sets to accurately evaluate its performance.

DISCUSSION

In this section, we present some discussion about the advantages and disadvantages or issues of the proposed method. The merits of the proposed method are (1) that it is very simple to implement compared to the conventional method and (2) that the noise prediction for a CSG can be efficiently performed since only the data from that CSG are needed unlike the conventional method that required many CSGs to be loaded into the computer memory. Despite of these advantages, the proposed method still has some issues that need be solved. The first issue is that the position of the reference near-offset geophone strongly affects the quality of the prediction. This is sensible since each trace has a different signal-to-noise ratio. To successfully apply the proposed method, a good reference trace is needed. This requires the processing person to judge and to choose the referene trace. The second issue is that noise in near-offset traces from source to the reference geophone are not predicted and thus not reduced. However, this is only a few near-offset traces.

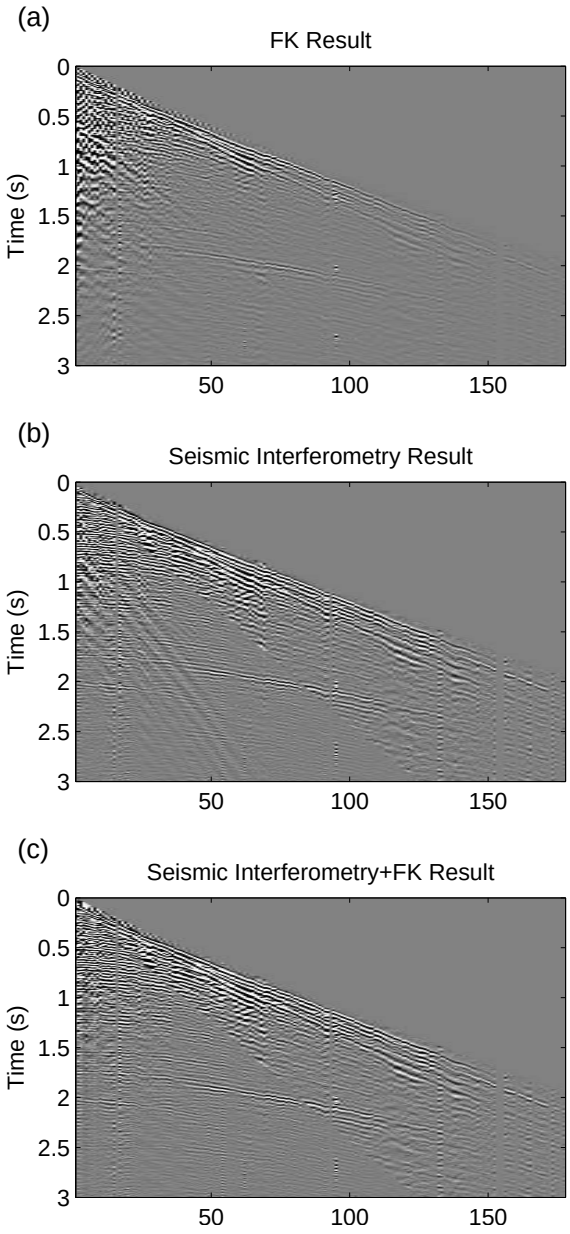

Figure 4: Comparison of filtering results obtained using three methods: (a) FK filtering, (b) new seismic interferometry filtering, and (c) hybrid between the new seismic interferometry and FK filtering.

CONCLUSION

A new method has been developed based on the principle of seismic interferometry for reducing strong surface-wave noise in land seismic data. The proposed method was applied to a 2D real surface-seismic-profile (SSP) data from PTTEP acquired in a north-east area of Thailand. A comparison with FK filtering shows that the proposed method is more effective but it still could not completely remove the surface-wave noise. FK filtering was then applied to the filtering result of the new seismic interferometry method to remove the residual noise. This hybrid was shown to be quite effective in reducing the noise from the data used in this paper. Nonetheless, more data sets should be used to test the performance of the proposed hybrid method.

ACKNOWLEDGMENTS

We would like to thank PTTEP for the financial support and the land seismic data used in this project.

REFERENCES

Bharadwaj, P., G. T. Schuster, I. Mallinson, and W. Dai, 2012, Theory of supervirtual refraction interferometry: Geophysical Journal International, **188**, no. 1, 263–273.

Halliday, D., A. Curtis, J. A. Robertsson, and D. V. Manen, 2007, Interferometric surface-wave isolation and removal: Geophysics, **72**, A69–A73.

Halliday, D., A. Curtis, P. Vermeer, C. Strobbia, A. Glushchenko, D. V. Manen, and J. A. Robertsson, 2010, Interferometric ground-roll removal: Attenuation of scattered surface waves in single-sensor data: Geophysics, **75**, SA15–SA25.

Mallinson, I., P. Bharadwaj, G. T. Schuster, and H. Jakubowicz, 2011, Enhanced refractor imaging by supervirtual interferometry: Leading Edge, **30**, no. 5, 546–550.

Xue, Y., 2010, Least squares datuming and surface waves prediction with interferometry: PhD thesis, University of Utah.

Xue, Y., S. Dong, and G. T. Schuster, 2009, Interferometric prediction and subtraction of surface waves with a nonlinear local filter: Geophysics, **74**, no. 1, SI1–SI8.

Surface-wave noise prediction using elastic waveform modeling

Jaroon Sinsawasmongkol and Chaiwoot Boonyasiriwat

ABSTRACT

...

INTRODUCTION

...

REFERENCES

A Fortran 90 Implementation of Matching Filter

Chaiwoot Boonyasiriwat

ABSTRACT

...

INTRODUCTION

...

REFERENCES

Part II

Migration and Inversion

Kirchhoff Full-Waveform Inversion

Chaiwoot Boonyasiriwat

ABSTRACT

...

INTRODUCTION

...

ACKNOWLEDGEMENTS

We are grateful for the support from PTTEP.

REFERENCES

Visco-acoustic full-waveform inversion in the space-frequency domain

Apirujee Nakpathom and Chaiwoot Boonyasiriwat

ABSTRACT

Full waveform inversion (FWI) is a method for estimating the physical properties of the Earth's subsurface structures from recorded geophysical data. Typically, FWI estimates a model of subsurface properties in an iterative manner by minimizing the misfit between predicted and recorded data. The predicted data are generated from a modeling process based on the visco-acoustic wave equation in the frequency-space domain. This is equivalent to solving a nonlinear inverse problem using an optimization technique. In this work, we use the L-BFGS quasi-Newton method for optimization, and develop a Fortran90 implementation of visco-acoustic FWI to estimate seismic velocity and quality factor (Q-factor) of the subsurface structure. The code was validated by the synthetic data experiment with the velocity and Q-factor models from Kamei and Pratt (2013). For the models, 2D elastic data were synthetically generated in the time domain using the Sofi2D. The frequency-domain data were then inverted for velocity and Q-factor models by visco-acoustic FWI. The numerical results show that velocity and Q-factor can be estimated from this algorithm, and the estimation is better for velocity than for Q-factor. In the future, we will conduct experiments on real seismic data.

INTRODUCTION

In seismic exploration, seismic waves were generated by artificial energy sources, and travel through the earth's subsurface. The waves reflect at boundaries where there are contrasts in acoustic impedance. These reflected and other waves are recorded by receivers on the surface - seismic data.

Full waveform inversion (FWI) is a method to estimate the subsurface property by matching the observed data and predicted data which are generated from a modeling process based on the visco-acoustic wave equation. Visco-acoustic FWI can estimate both the velocity and quality factor of the subsurface. Attenuation is a mechanism that decreases the amplitude of seismic waves propagating through the medium. The real earth attenuates waves due to the conversion of wave energy into heat. This an-elastic behavior decease amplitude of the wave field and thus can have effect on FWI by reducing the resolution of the estimated model. So it is important to compensate for an-elastic behavior to make the estimated results more reliable. Attenuation properties of the subsurface can be expressed as quality factor (Q), a dimensionless value that involves with wave velocity as the complex velocity.

Visco-acoustic wave field that propagate through the earth can be generate by applying finite difference method (FDM) to acoustic wave equation, in this case, in frequency-space domain (FD). There are the advantages of the FDFDM wave modeling approach. For example, FDFDM modeling can be specified as a discrete matrix formulation, so it is possible to derive matrix formulas for the iterative non-linear inverse method, i.e. steepest descent method and Gauss-Newton method. It also allows us to sequential reconstruct model parameters from low to high frequency component of the data. Different from time domain inversion methods that use all frequency of the data, frequency domain methods use only few frequencies to invert the accurate model. By using the low frequency estimated model as a starting model for later inversions, the chance of convergence to a local minimum is somewhat reduced. Furthermore, the attenuation can be included at no increased computational cost by straight forward using the complex velocity. In contrast, time domain methods require convolution operation with a response function to model visco-acoustic effects. Another advantage is the simultaneously multisource modeling by using LU decomposition. Use of LU decomposition in FDFDM allows the fast calculation of the wavefield due to multiple sources once an initial factorization step is completed.

In this study, we developed the modeling and inver-

sion code. The code is written in Fortran 90 as the subprogram in Madagascar and uses Message Passing Interface (MPI) and OpenMP for parallelism. We also use the MUlti frontal Massively Parallel direct Solver (MUMPS) for solving LU factorization.

In theory section, we present the mathematical method used in visco-acoustic modeling and inversion. The two-difference minimization method, i.e. steepest descent and Quasi-Newton, will be introduced. The FWI algorithm is also presented as flow chart in this section.

In synthetic results section, we investigated the minimization scheme by testing with the complex model from Kamei and Pratt 2013. The synthetic data are generated with 3 difference method such as a visco-acoustic finite difference in frequency domain (same algorithm to calculate the culcated data in the inversion process), a visco-acoustic finite difference in time domain and a visco-elastic finite difference in time domain. We use the external package (Sofi2D) to generate the last two sets of data. the results show that the algorithm can estimate both velocity and quality factor from all data set, but velocity estimated form visco-elastic data set has a lower resolution compare with another data set, because it contain the s-wave in data that will be classified a noise.

In the results from real field data,

THEORY

Visco-acoustic Wave Modeling in Frequency Domain

From the two-dimensional acoustic wave equation in space-time domain,

$$1c(x,z)^2\partial^2\partial t^2 p(x,z,t)+\left[\partial^2\partial x^2+\partial^2\partial z^2\right]p(x,z,t)=s(x,z,t) \tag{1}$$

where $p(x,z,t)$ is the pressure wavefield, $s(x,z,t)$ is source, and $c(x,z)$ is acoustic wave velocity. We apply Fourier transform to equation (1), and then we obtain

$$\omega^2 c(x,z)^2 P(x,z,\omega)+\left[\partial^2\partial x^2+\partial^2\partial z^2\right]P(x,z,\omega)=S(x,z,\omega) \tag{2}$$

Above equation is the two-dimensional acoustic wave equation in the space-frequency domain. Where $P(x,z,\omega)$ and $S(x,z,\omega)$ is the pressure wavefield and source in the space-frequency domain. ω is the angular frequency.

One of the advantage of working in the frequency domain is we can directly implement of the attenuation property through the relation

$$\tilde{c}=c\left[1+i2Q\right]^{-1} \tag{3}$$

where $\tilde{c}$ is the complex velocity and Q is the attenuation factor.

In order to solve Eq. (2), we discretize equation (2) using an implicit finite difference scheme based on 4^{th} order finite difference method. At the boundary of the computational domain, we use the perfectly matched to absorb wave energy at outside the computational domain.

From the discretization, acoustic wave equation (2) can be written in a matrix form as,

$$\mathbf{A}(\mathbf{m})\mathbf{p}=\mathbf{s} \tag{4}$$

Where $\mathbf{A}$ is the sparse differential operators matrix with dimension $N\times N$, where $N=nz\times nx$, depends on frequency ω and on model properties $\mathbf{m}$ that includes both velocity and attenuation variation. Two-dimensional pressure $\mathbf{p}$ and source $\mathbf{s}$ fields at frequency ω are stored as vectors of dimension N.

The 2D pressure field is obtained by solving the system of linear equation, eq.8. In this study, MUMPS (MUltifrontal Massively Parallel sparse direct Solver) is used to solve the equation. Therefore, multiple sources' solutions can be obtained once the matrix $\mathbf{A}$ was factorized using a $\mathbf{LU}$ decomposition scheme:

$$\mathbf{LU}\left[\mathbf{p}_1\mathbf{p}_2\ldots\mathbf{p}_{ns}\right]=\left[\mathbf{s}_1\mathbf{s}_2\ldots\mathbf{s}_{ns}\right] \tag{5}$$

This is the other advantage of working in the frequency domain, because we can simulation the wavefield from multi-source simultaneously.

Full-waveform Inversion Algorithm

The least-squares misfit function that is minimized is given by

$$E(\mathbf{m})=12\triangle\mathbf{d}^{\dagger}\triangle\mathbf{d} \tag{6}$$

where $\triangle\mathbf{d}$ is the data residual vector, $\triangle\mathbf{d}=\mathbf{d}_{obs}-\mathbf{d}_{cal}(\mathbf{m})$, the difference between observed and calculated data. The symbol † denotes the complex conjugate operator.

From a starting model $\mathbf{m}_0$, we are going to search for a local minimum of the misfit function $E(\mathbf{m}_0)$ by iterative nonlinear local optimization. By following the Born approximation (Born and Wolf (1993); Beydoun and Tarantola (1988)), The estimated model $\mathbf{m}$ can be written as $\mathbf{m}=\mathbf{m}_0+\triangle\mathbf{m}$, where $\triangle\mathbf{m}$ is a perturbation model.

The misfit function of model $\mathbf{m}$, $E(\mathbf{m})$, can be expanded by Taylor series as,

$$E(\mathbf{m}_0+\triangle\mathbf{m})=E(\mathbf{m}_0)+\sum_{j=1}^{M}\partial\mathrm{E}(\mathbf{m}_0)\partial m_j\triangle m_j+12\sum_{j=1}^{M}\sum_{k=1}^{M}\partial^2\mathrm{E}(\mathbf{m}_0)\partial \tag{7}$$

Where M denotes the number of inverted parameter. The first order derivative respect to the model parameter m_l can be written as,

$$\partial\mathrm{E}(\mathbf{m})\partial m_l=\partial\mathrm{E}(\mathbf{m}_0)\partial m_l+\sum_{j=1}^{M}\partial^2\mathrm{E}(\mathbf{m}_0)\partial m_j\partial m_l\triangle m_j \tag{8}$$

The misfit function reaches its minimum when the first order derivative equal zeros. Therefore, the left hand term

must be set to zero,

$$0 = \partial \mathrm{E}(\mathbf{m}_0)\partial m_l + \sum_{j=1}^{M} \partial^2 \mathrm{E}(\mathbf{m}_0)\partial m_j \partial m_l \triangle m_j \qquad (9)$$

And implies this expression respect to model parameter $\mathbf{m}$,

$$-\partial \mathrm{E}(\mathbf{m}_0)\partial \mathbf{m} = \partial^2 \mathrm{E}(\mathbf{m}_0)\partial \mathbf{m}^2 \triangle \mathbf{m} \qquad (10)$$

Hence, the perturbation model:

$$\triangle \mathbf{m} = -\left[\partial^2 \mathrm{E}(\mathbf{m}_0)\partial \mathbf{m}^2\right]^{-1} \partial \mathrm{E}(\mathbf{m}_0)\partial \mathbf{m} \qquad (11)$$

where $\partial \mathrm{E}(\mathbf{m}_0)\partial \mathbf{m}$ is called the gradient $\nabla \mathrm{E}(\mathbf{m}_0)$ and $\partial^2 \mathrm{E}(\mathbf{m}_0)\partial \mathbf{m}^2$ the Hessian $\mathcal{H}$.

Gradient expression

For multiple sources and frequencies, The gradient of the misfit function for the model parameter m_j is computed with the adjoint-state method (Chavent (1974); Tarantola (1984); Plessix (2006); Chavent (2009)), which gives

$$\nabla E_{m_j} = -\sum_{k=1}^{N_\omega}\sum_{l=1}^{N_s} \mathbb{R}\left[\mathbf{p}_{l,k}^T \left(\partial \mathbf{A}_k \partial m_j\right)^T \mathbf{A}_k^{-1} \triangle \mathbf{d}_{l,k}^*\right] = -\sum_{k=1}^{N_\omega}\sum_{l=1}^{N_s} \mathbb{R}\left[\mathbf{p}_{l,k}^T \left(\partial \mathbf{A}_k \partial m_j\right)^T \mathbf{r}_{l,k}^*\right] \qquad (12)$$

where ^{T} denotes the transpose operator, * the complex conjugate,N_s the number of sources, and N_ω the number of frequencies simultaneously inverted, in this case, $N_\omega = 1$. $\mathbb{R}$ defines the real part of the complex value $\mathbf{p}_{l,k}$ is the monochromatic incident wavefield associated with frequency k and source l. $\mathbf{r}_{l,k}$ is the back-propagated residual wavefield. Note that the residuals associated with one source are assembled to from one vector.

Hessian expression

The Hessian reads

$$\mathcal{H} = \mathbb{R}\left[\mathbf{J}^T\mathbf{J}^*\right] + \mathbb{R}\left[(\partial \mathbf{J}\partial \mathbf{m})^T (\delta \mathbf{d}^* \cdots \delta \mathbf{d}^*)\right] \qquad (13)$$

where $\mathbf{J}$ is the Frechet derivative or the sensitivity matrix. The first term $\mathbb{R}\left[\mathbf{J}^T\mathbf{J}^*\right]$ is called the approximate Hessian. It is the zero-lag correlation between the partial derivative of wavefields with respect to different parameters. Therefore, it represents the spatial correlation between the images of different point scatterers. It can be view as a resolution operator resulting from limited bandwidth of the source and the acquisition geometry. Indeed, applying the inverse of the Hessian is equivalent to applying a spiking deconvolution of the gradient misfit function. (e.g. Ali et al. (2009))

The term $\mathbb{R}[\mathbf{J}^T\mathbf{J}^*]$ is diagonal dominant since the diagonal terms are defined by zero-lag auto-correlation. This diagonal term reduces the effects of the geometrical spreading. Therefore, in the frame of surface acquisition, it helps to scale the deep perturbations (large offsets / small amplitudes) with respect to the shallow perturbations (near offsets / high amplitudes)

The second term $\mathbb{R}\left[\left(\frac{\partial \mathbf{J}}{\partial \mathbf{m}}\right)^T (\delta \mathbf{d}^* \cdots \delta \mathbf{d}^*)\right]$ is the zeros-lag correlation between the second-order partial derivative of the wavefields with data residuals. Since first-order partial derivative os related to single scattering, it can be expected that second-order partial derivative is related to double or multiple scattering.

The perturbation model (descent direction) equation (15) reads

$$\triangle \mathbf{m} = \left\{\mathbb{R}\left[\mathbf{J}^T\mathbf{J}^* + (\partial \mathbf{J}\partial \mathbf{m})^T (\delta \mathbf{d}^* \ldots \delta \mathbf{d}^*)\right]\right\}^{-1} \nabla E_{\mathbf{m}} \qquad (14)$$

This expression is generally referred as the Newton method, which is locally quadratic convergence.

Generally, the second term of Hessian is neglected since in the framework of the Born approximation multiple scattering are neglected (Pratt et al. (1998)). This leads to a quasi-Newton direction called Gauss-Newton,

$$\triangle \mathbf{m} = \left\{\mathbb{R}\left[\mathbf{J}^T\mathbf{J}^*\right]\right\}^{-1} \nabla E_{\mathbf{m}} \qquad (15)$$

If the Hessian is replaced by a scalar α, the expression gives the steepest descent direction,

$$\triangle \mathbf{m} = \alpha \nabla E_{\mathbf{m}} \qquad (16)$$

Consider the approximate Hessian $\mathcal{H}_a$ (Pratt et al. (1998)) defined by

$$\mathcal{H}_a = \mathbb{R}\left[\mathbf{J}^T\mathbf{J}^*\right] \qquad (17)$$

The element of the Frechet derivative matrix associated with the source-receiver pair k and the parameter m_j is given by (Ali et al. (2009); Malinowski et al. (2011))

$$\mathbf{J}_{k(s,r),l} = \mathbf{p}_s^T \left(\partial \mathbf{A} \partial m_j\right)^T \mathbf{A}^{-1} \delta_r \qquad (18)$$

where δ_r is an impulse source located at the receiver position r. As shown by the equation above, we have to simulate one forward problem for each source and each receiver pair. This means that the computational cost of the approximate Hessian depends on the acquisition geometry and number of sources and receivers. In the huge acquisitions, the large space of the storage must be required for the approximate Hessian.

To mitigate the problem, only diagonal terms of the approximate hessian are computed at first iteration of the inverted frequency (Ravaut et al. (2004); Operto et al. (2006)).

To update the approximate Hessian or its inverse $\mathcal{H}^{(i)}$ at each iteration of inversion, the BFGS algorithm is applied by taking into account the additional knowledge of $\nabla E^{(i)}$ at iteration i. The BFGS formula for the inverse of the quasi-Hessian is given by,

$$\mathcal{H}_{(i+1)}^{-1} = \left(\mathbf{I} - \mathbf{s}_i\mathbf{y}_i^T\mathbf{y}_i^T\mathbf{s}_i\right)\mathcal{H}_{(i)}^{-1}\left(\mathbf{I} - \mathbf{y}_i\mathbf{s}_i^T\mathbf{y}_i^T\mathbf{s}_i\right) + \mathbf{s}_i\mathbf{s}_i^T\mathbf{y}_i^T\mathbf{s}_i \tag{19}$$

where $\mathbf{s}_i = \mathbf{m}_i - \mathbf{m}_{(i-1)}$ and $\mathbf{y}_i = \nabla E_{(i)} - \nabla E_{(i-1)}$. In this study, we used only the diagonal part of the hessian.

RESULTS

Results from Synthetic data

In synthetic experiment, we use the velocity and Q-factor models from Kamei and Pratt (2013). There models are interesting in that 3 velocity zone and non-corresponding 3 Q-factor zone. There are also a lot of detail in this model that challenge us to recover the detail.

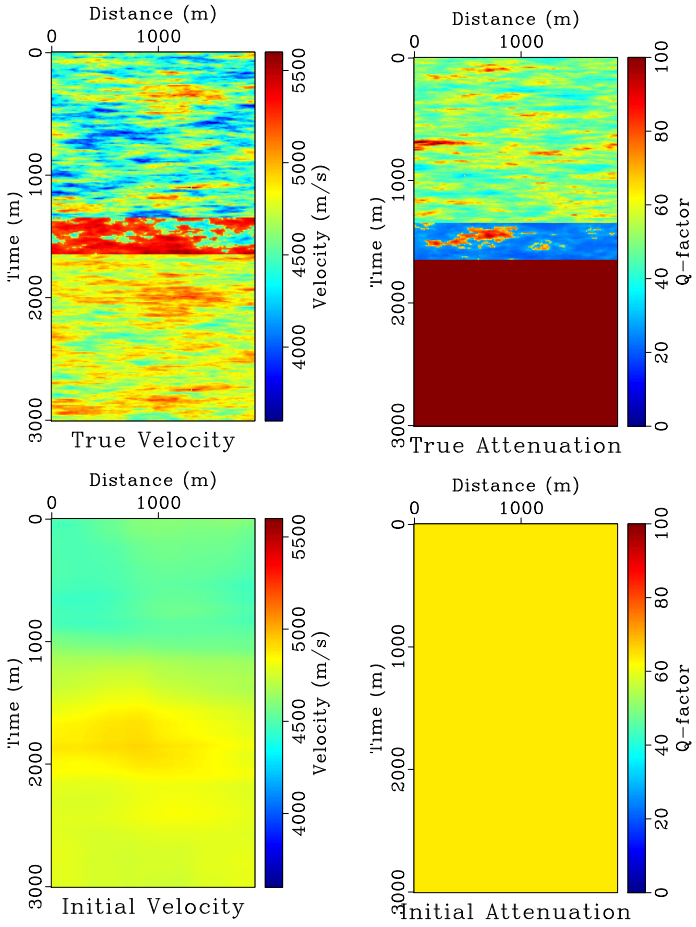

The acquisition geometry is shown in 1. From the initial model, we inverted to find the estimated model with 24 frequency components start from 3 to 49 Hz with 2 Hz interval.

We generated 3 observed data sets from the same true model. The first one is the visco-acoustic data from frequency-domain finite difference which is a same modelling algorithm using in the inversion process. The other 2 types are the visco-acoustic and visco-elastic data that obtain from time-domain finite difference modelling from Sofi2D package.

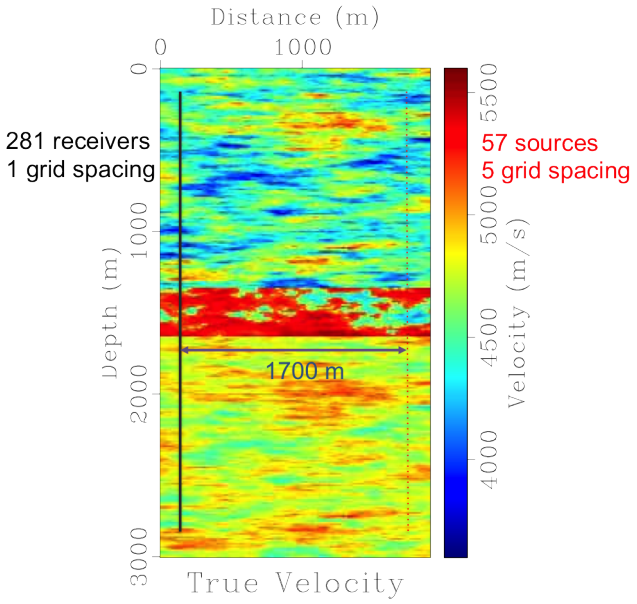

Figure 1: Acquisition

In this test, In case of onshore, receivers locate at 25 m depth. Frequency components between 1 and 30 Hz are fully inverted. We used the algorithms that present in Figure 2 but instead of converting complex slowness, v-q parameters are inverted, and had results as shown in table 1.

Results from Field data

In this test, we applied the algorithm with the field data set. There are 14 total shot with the hand correct trace used. The results show in table 2.

SUMMARY

Both velocity and attenuation can be reconstructed by FWI without the constrain of maximum and minimum value of the model. From the estimated model form synthetic data, we can see that,not only the structure, but also the value of velocity and Q-factor were accurately estimated. Even though there are the shear wave component in the visco-elastic data, we still can find the rough structure of the model accurately.

ACKNOWLEDGMENTS

The authors are grateful for the support from PTTEP for the Mahidol University Center for Scientific Computing (MCSC).

REFERENCES

Ali, H. B. H., S. Operto, and J. Virieux, 2009, Efficient 3d frequency-domain full waveform inversion (fwi) with phase encoding, *in* 71st EAGE Conference & Exhibition, SPE and EAGE.

Beydoun, W. and A. Tarantola, 1988, First born and rytov approximations: Modeling and inversion conditions in a canonical example: Journal of the Acoustical Society of America, **83**.

Born, M. and E. Wolf, 1993, Principles of optics: Electromagnetic theory of propagation, interference and diffraction of light; sixth edition with corrections: Pergamon Press.

Chavent, G., 1974, Identification of functional parameter in partial differential equations: Identification of Parameters in Distributed Systems, 31–48.

———, 2009, Non linear least squares for inverse problems. Scientific Computation: Springer.

Kamei, R. and R. Pratt, 2013, Inversion strategies for visco-acoustic waveform inversion: Geophysical Journal International, **194**, 859–884.

Malinowski, M., S. Operto, and A. Ribodetti, 2011, High-resolution seismic attenuation imageing from wide-aperture onshore data by visco-acoustic frequency-domain full-waveform inversion: Geophysical Journal International, **186**, 1179–1204.

Operto, S., J. Virieux, J.-X. Dessa, and G. Pascal, 2006, Crustal seismic imaging from multifold ocean bottom seismometer data by frequency domain full waveform tomography: Application to the eastern nankai trough: Journal of Geophysical Research: Solid Earth, **111**.

Plessix, R.-E., 2006, A review of the adjoint-state method for computing the gradient of a functional with geophysical applications: Geophysical Journal International, **167**, 495–503.

Pratt, R., C. Shin, and Hicks, 1998, Gauss–newton and full newton methods in frequency–space seismic waveform inversion: Geophysical Journal International, **133**, 341–362.

Ravaut, C., S. Operto, L. Improta, J. Virieux, A. Herrero, and P. Dell'Aversana, 2004, Multiscale imaging of complex structures from multifold wide-aperture seismic data by frequency-domain full-waveform tomography: application to a thrust belt: Geophysical Journal International, **159**, 1032–1056.

Tarantola, A., 1984, Inversion of seismic reflection data in the acoustic approximation: Geophysics, **49**, 1259–1266.

F90-MADAGASCAR VISCO-ACOUSTIC FWI CODE FLOWCHART

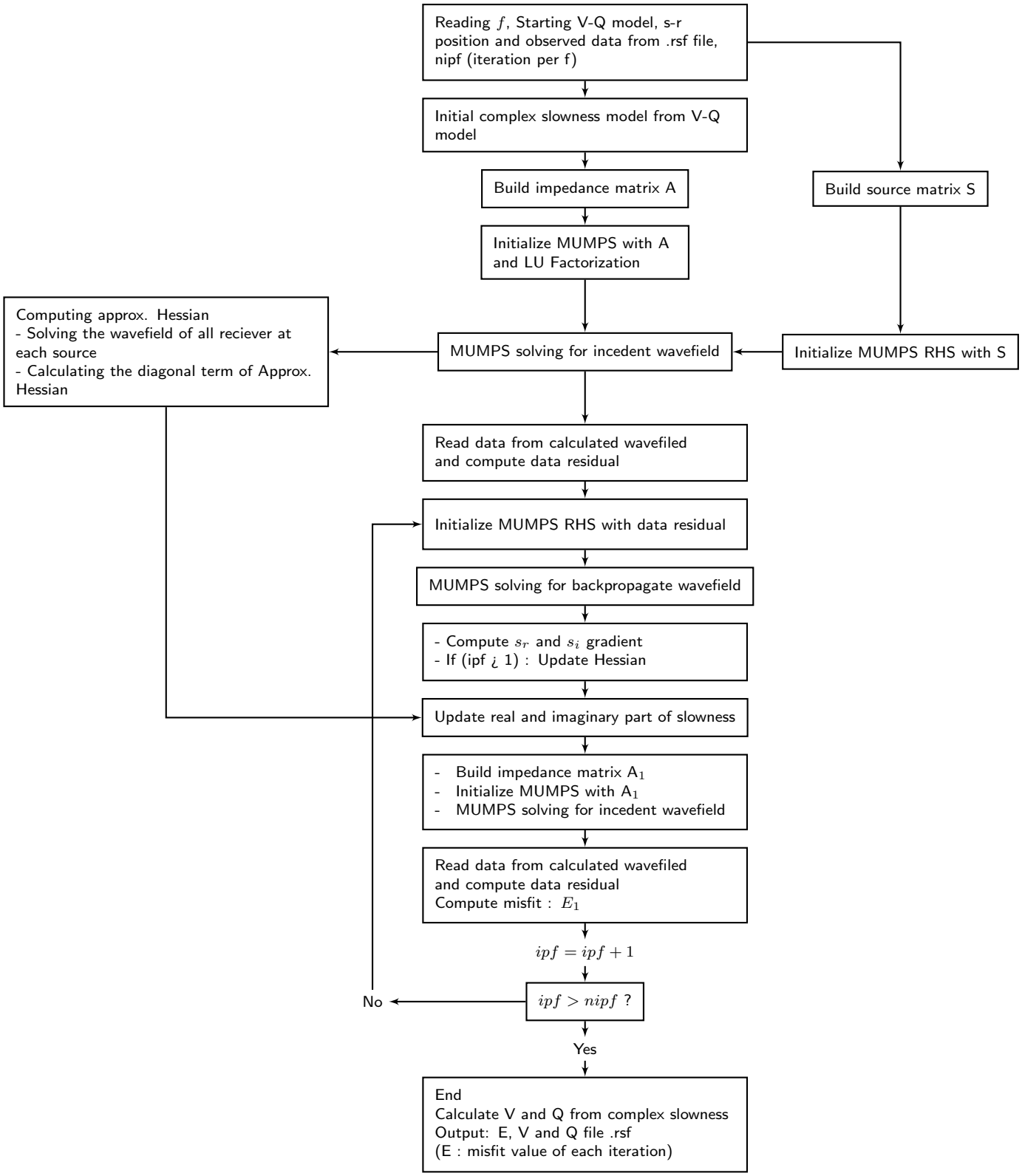

Figure 2: F90-Madagascar Inversion Code Flow Chart

Table 1: Comparing between Steepest descent with v-q parameter and quasi-Newton with complex slowness parameter

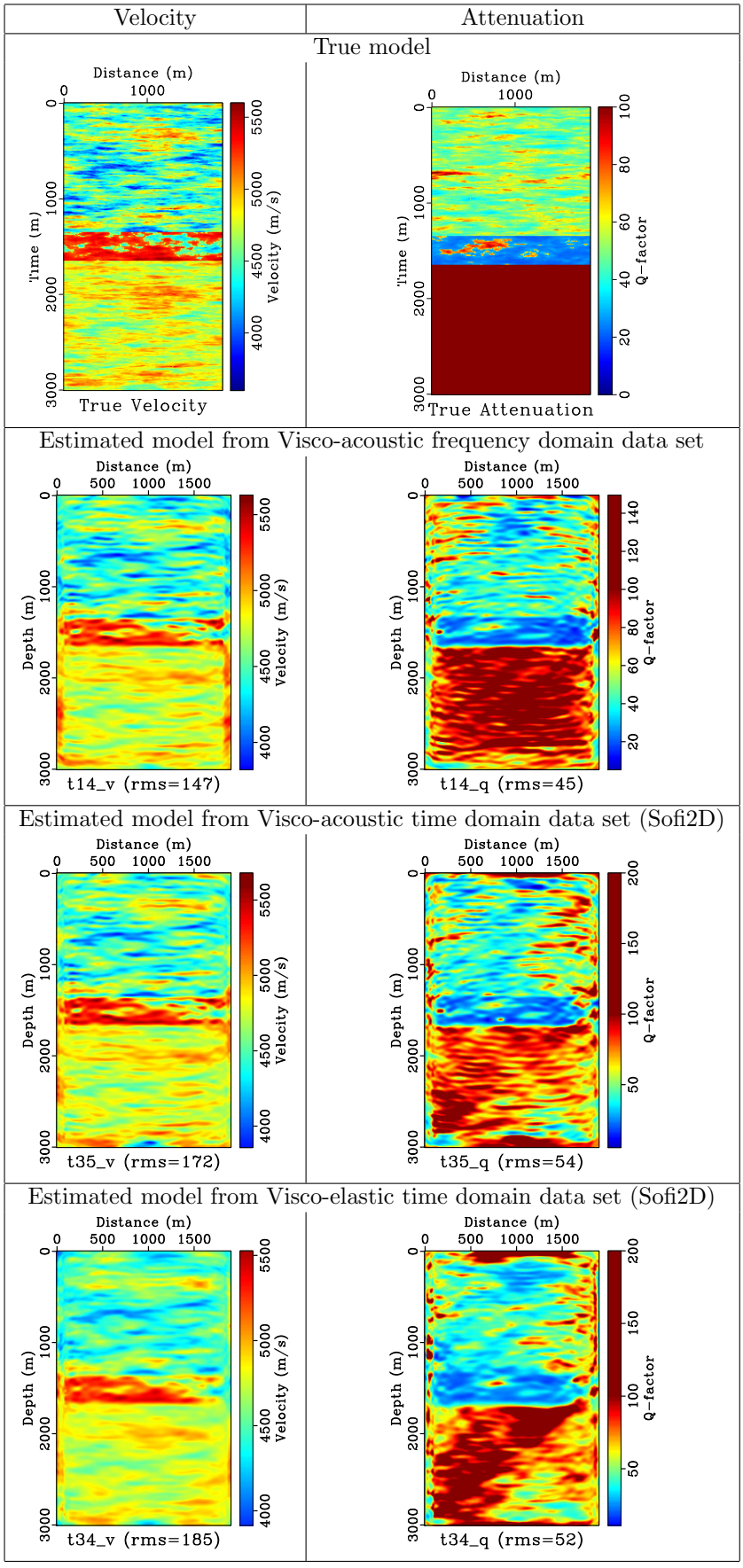

Table 2: Comparing between Steepest descent with v-q parameter and quasi-Newton with complex slowness parameter

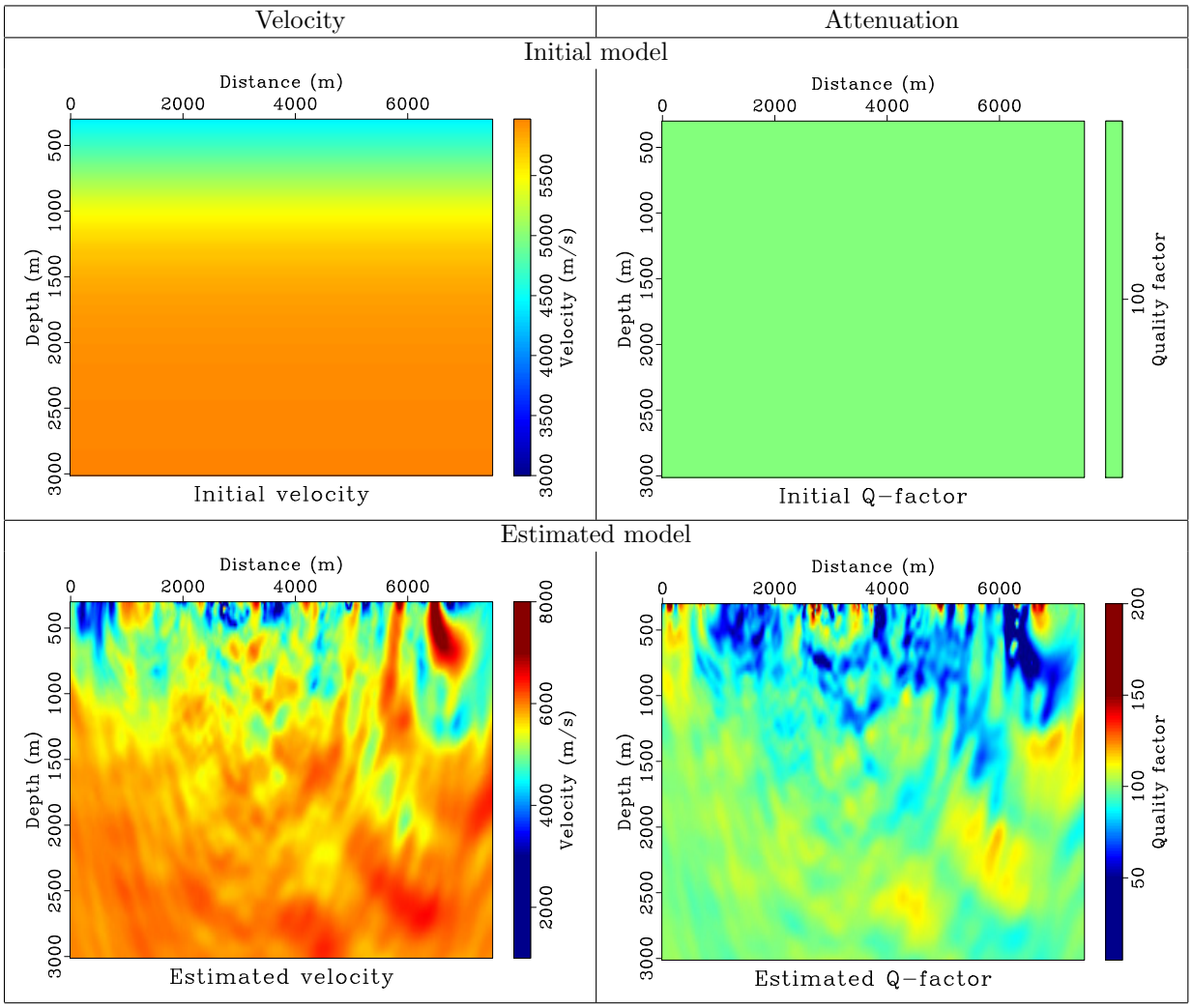

Kirchhoff Prestack Depth Migration of 2D Isan Land Data

Chaiwoot Boonyasiriwat

ABSTRACT

...

INTRODUCTION

...

ACKNOWLEDGEMENTS

We are grateful for the support from PTTEP.

REFERENCES

Part III

Software Development

Computer Physics Communications
1,2]Chaiwoot Boonyasiriwat 3]Gerard T. Schuster 2]Weerachai Siripunvaraporn

1]Mahidol University Center for Scientific Computing, Department of Physics, Faculty of Science, Mahidol University, Bangkok, Thailand 2]Geophysics Research Group, Department of Physics, Faculty of Science, Mahidol University, Bangkok, Thailand 3]Center for Seismic Imaging and Fluid Modeling, King Abdullah University of Science and Technology, Thuwal, Kingdom of Saudi Arabia

MMI2D: Two-dimensional modeling, migration, and inversion program for seismic data analysis

[

ABSTRACT

Seismic reverse-time migration (RTM) and full-waveform inversion (FWI) are high-resolution methods that have been recently widely used in the seismic exploration industry. Many computer program have been developed and commercialized but there are only a few public-domain programs including FWT2D, a frequency-domain full-waveform inversion program. To provide an alternative computational tool for reseachers and to promote the reproducibility of scientific research, we present a computer program named MMI2D that is capable of performing two-dimensional seismic modeling, migration, and inversion in the time domain based on the acoustic wave equation. In the program, an explicit finite-difference method was used to numerically solve the wave equations, and the adjoint-state method was used for model parameter estimation in RTM and FWI. In addition, multiscale, multisource, and regularization methods were utilized to improve computational efficiency and robustness of the program. Detailed descriptions of MMI2D were given and to demonstrate its use numerical results are also presented.

reverse-time migration, full-waveform inversion multiscale multisource regularization

INTRODUCTION

Reverse-time migration (RTM) and full-waveform inversion (FWI) are seismic methods based on the wave equation for estimating physical properties of the Earth's subsurface structures. Despite their high computational costs, there still be a strong interest in both methods due to their ability to provide a high-resolution image of the subsurface structures which is crucial for an accurate and reliable interpretation for potential reservoirs of natural resources such as petroleum and ores.

Both RTM and FWI have been implemented and commercialized by many companies. Only a few computer program were released in the public domain such as FWT2D which is a 2D FWI program in the frequency domain developed by Sourbier et al. (2009). As to out best knowledge, there is no non-commerical software for time-domain FWI. Therefore, we present here a computer program for 2D full-waveform inversion in the time domain to be an alternate research tool and to help promote the reproducibility of scientific research. The proposed program is named MMI2D due to its ability to perform seismic modeling, migration, and inversion in two dimensions. MMI2D was written in Fortran 90 programming language and used the message-passing interface (MPI) for parallel computation. In the modeling part, the acoustic wave equation is numerically solved using and explicit finite-difference method with a free-surface boundary at the top surface and absorbing boundaries at the other boundaries. Forward modeling is a crucial part of reverse-time migration (RTM) and full-waveform inversion (FWI), and also is the most time-consuming part of RTM and FWI. The computational efficiency of RTM and FWI can be improved by using the adjoint-state method Tarantola (1984) and the multisource method Krebs et al. (2009); Schuster et al. (2011) while the local minima and nonuniqeness problems were partially solved by using the multiscale and regularization methods.

We begin by describing the details of seismic modeling followed by reverse-time migration and full-waveform inversion. Then we describe how to use the software with some numerical examples. Finally, a summary is given with the future work.

THEORY AND IMPLEMENTATION

Seismic Modeling

In MMI2D, seismic waves were assumed to be propagating in isotropic media in the x-z plane and governed by

the acoustic wave equation. Two types of acoustic wave equation can be used for seismic modeling: the constant-density acoustic wave equation, given by

$$\frac{1}{v^2(x,z)}\frac{\partial^2 p(x,z,t)}{\partial t^2} - \frac{\partial^2 p(x,z,t)}{\partial x^2} - \frac{\partial^2 p(x,z,t)}{\partial z^2} = s(x,z,t), \tag{1}$$

and the variable-density acoustic wave equation, given by

$$\begin{aligned}
\frac{\partial p(x,z,t)}{\partial t} &= -\frac{1}{\kappa(x,z)}\left[\frac{\partial v_x(x,z,t)}{\partial x} + \frac{\partial v_z(x,z,t)}{\partial z}\right] + s'(x,z,t), &(2)\\
\frac{\partial v_x(x,z,t)}{\partial t} &= -\frac{1}{\rho(x,z)}\frac{\partial p(x,z,t)}{\partial x}, &(3)\\
\frac{\partial v_z(x,z,t)}{\partial t} &= -\frac{1}{\rho(x,z)}\frac{\partial p(x,z,t)}{\partial z}, &(4)
\end{aligned}$$

where $p(x,z,t), v_x(x,z,t)$, and $v_z(x,z,t)$ are the pressure, horizontal, and vertical particle velocities, respectively, at position (x,z) at time t, κ is the bulk modulus, ρ is the density, $v = \sqrt{\kappa/\rho}$ is the velocity, s and s' are the source functions. In this work, we assume that the source is a point source, i.e., $s(x,y,t) = \delta(x-x_s, z-z_s)S(t)$ and $s'(x,z,t) = \delta(x-x_s, z-z_s)S'(t)$ where (x_s, z_s) is the source position, and $S(t)$ and $S'(t)$ are the source time functions.

The constant- and variable-density acoustic wave equations are numerically solved using the explicit finite difference method with standard and staggered grids, respectively. The finite-difference coefficients used in MMI2D are those of the optimized finite-difference operator proposed by (Zhang and Yao, 2013,Table 1). The time integration is approximated by a finite difference method and has an accuracy of second order in both cases.

The image method 3 proposed by Robertsson (1996) was used to implement the free-surface boundary condition at the top surface, and perfectly matched layer (PML) was used to reduce spurious reflections from the other domain boundaries. The PML versions of the wave equations used in MMI2D are shown in Appendix A.

Reverse-Time Migration and Full-Waveform Inversion

Reverse-time migration (RTM) is a seismic migration method based on the two-way wave equation and, therefore, is more accurate than migration methods based on the ray theory and one-way wave equation such as Kirchhoff migration and phase-shift migration. RTM can be thought of as one iteration of full-waveform inversion although the input of RTM is the observed seismic data while that of FWI is the difference between the observed and predicted data or data misfit. Nevertheless, we will only describe briefly the theory of full-waveform inversion in the time domain.

In MMI2D, full-waveform inversion can estimate the physical properties of the subsurface structures by minimizing the objective function

$$E(\mathbf{m}) = ||\mathbf{d}_{pre} - \mathbf{d}_{obs}||^2 + \lambda||L\mathbf{m}||^2 \tag{5}$$

where $\mathbf{d}_{pre} = A(\mathbf{m})$ and $\mathbf{d}_{obs}$ are the predicted and observed data, A is the forward modeling operator depending on the numerical method used to solve the wave equation, λ is the regularization parameter or Lagrange multiplier, L is the roughness operator, and $\mathbf{m}$ is the model of physical properties. Typically, gradient-based optimization methods are used to minimize the objective function. In MMI2D, the steepest descent and conjugate gradient methods can be used for optimization. The computation of the gradient of the objective function is efficiently performed using the adjoint-state method Tarantola (1984); Boonyasiriwat et al. (2009). The model is iteratively updated using the model update equation

$$\mathbf{m}_{i+1} = \mathbf{m}_i + \alpha\mathbf{l}, \tag{6}$$

where $\mathbf{m}_i$ is the i-th iterate of the model parameter, α is the step length, and $\mathbf{l}$ is the line-search direction depending on the optimization used. In MMI2D, a quadratic interpolation method was used to find an optimal or near-optimal step length for each line search Vigh and Starr (2008).

The main issues of FWI include the high computational cost, many local minima and the non-uniqueness of the solution. FWI is computationally intensive due to the large number of forward modeling needed during the inversion. The last two issues came from the fact that FWI is an ill-posed nonlinear inverse problem. In addition to the adjoint-state method, MMI2D utilizes the multisource inversion Krebs et al. (2009); Schuster et al. (2011) to increase the computational efficiency. The time-domain multiscale inversion Boonyasiriwat et al. (2009); Bunks et al. (1995) was used to partially overcome the local minima problem. Smoothness-constrained regularization was utilized to solve the non-uniqueness problem. This is equivalent to using the Occam's principle to seek the simplest solution that can explain the data.

USAGES OF MMI2D

To use MMI2D, an additional input file is required. This file is an ASCII file that contains parameters for each type of computation. These parameters are categorized into two types: required and optional parameters.

Forward Modeling

Forward modeling can be performed by solving either the constant- or variable-density acoustic wave equation. Once the type of equation is selected, a finite-difference grid is automatically chosen as described in the Forward Modeling section. The user can choose the order of the finite-difference scheme by setting the parameter "fd_order". In addition to the parameters for the finite-difference solver, the user need to provide information about the velocity

and/or density models, source and receiver locations, and source time function. Optional parameters include the output file location, the thickness of the PML region, the type of surface boundary condition, and the amount of random noise to be added to the output seismogram.

Here is an example of the input parameter file.

```
jobtype=modeling        # type of computation
gridtype=standard       # type of finite-difference grid
fd_order=4              # the order of finite-difference scheme
velfile_in=vel.dat      # velocity model file in binary format
densityfile=n/a         # density model file in binary format
topofile=n/a            # topography file in binary format
coordfile=coord.dat     # ASCII file containing sources and receiver locations
nx=501                  # number of model points along the x axis
nz=401                  # number of model points along the z axis
dx=10.0                 # spatial sampling interval in both x and z directions
nt=4001                 # number of time samples
dt=0.001                # temporal sampling interval
freq=10.0               # peak frequency of Ricker source wavelet
sourcefile=n/a          # input file for the source time function
csg_out_prefix=csg      # file prefix for the output data
npml=50                 # thickness of the PML region in unit of grid points
noise_level=0           # random noise level in the output data
free_surface=1          # type of boundary condition at the surface
```

In the input file, the following parameters are the required parameters.

- "jobtype=mod": Type of computation is forward modeling
- "velfile=vel.dat": Binary file containing the velocity model
- "coordfile=coord.dat": ASCII file containing the locations of sources and receivers. Each line must contains 7 columns. The first two columns are the source and receiver indices, respectively. The third and fourth columns are the source location in the x- and z-directions whilse the fifth and sixth columns are the receiver location in the x- and z-directions. The last column is the first-arrival traveltimes which is reserved for early-arrival full-waveform inversion Sheng et al. (2006); Boonyasiriwat et al. (2010). In this case, the last column is not used and can be set to any number.
- "nx=501" and "nz=401": The number of model points along the x- and z-directions.
- "dx=10.0": The spatial sampling interval in both x- and z-directions are assumed to be the same in MMI2D and is in the unit of meter.
- "nt=4001": The number of time samples of the source function and also of the output data.
- "dt=0.001": The temporal sampling interval in seconds.
- "freq=10.0": The peak frequency of the Ricker source function is required when there is no input source file specified in the parameter "sourcefile".
- "sourcefile=n/a": "n/a" means there is no input source file. The user can replace "n/a" by the file name of the source file which is in the binary format.

Optional Parameters

The following parameters are optional.

- "gridtype=standard": Default finite-difference grid is the "standard" grid which corresponds to solving the constant-density acoustic wave equation. Another option is "staggered" grid which corresponds to solving the variable-density acoustic wave equations.
- "fd_order=4": The order of the optimized finite-difference scheme is by default set to 4. The available orders of the optimized FD scheme are 2, 4, 8, and 16.
- "densityfile=n/a": The density model file is not required for constant-density modeling but is required for variable-density modeling. The density model file must be in the binary format and the density model must have the same dimension as the velocity model.
- "topofile=n/a": The topography file is not required for modeling with a flat surface but is required for modeling with a rugged surface topography. The topography file must be in the binary format containing the elevation at each x position in the model.
- "csg_out_prefix=csg": The prefix of the output data file will be combined with shot number and file type. The actual output data will be saved as a separate common shot gather for each source, e.g., csg1.su.
- "npml=40": The thickness of the PML region is by default set to 40 grid points.
- "noise_level=0": The amount of random noise to be added to the output data is by default set to zero.
- "free_surface=1": This parameter is used to specified the type boundary condition at the surface. For the free surface boundary condition, this parameter must be equal to 1. To use PML, set this parameter to 0. For Neumann boundary condition, set this parameter to 2. By default, the free-surface boundary condition is used.

Reverse-Time Migration

The input parameters for conventional reverse-time migration are the same as in the forward modeling case except there is one more required parameter which is the input seismogram. The name of this parameter is "csg_in_prefix".

One more difference is in the value of the parameter "jobtype". In this case, set "jobtype=migration".

For multisource reverse-time migration, there are three more required parameters: "multisrc_file", "nsg", and "nss". The first parameter is the name of the binary file containing the random phase encoding information for multisource RTM. The second parameter is the number of supergather (nsg) while the last parameter is the number of simultaneous sources (nss). The random phase encoding information was generated using the Halton quasi-random number generator.

Full-Waveform Inversion

To run a full-waveform inversion job, the user needs set "jobtype=inversion". In this case, there are many more required parameters due to the complexity of full-waveform inversion. The required parameters include those for the multisource method and additional parameters for the regularized inversion process which are as followed.

- "itermax=10": the maximum number of iterations
- "vmin=1500.0" and "vmax=3500.0": the minimum and maximum velocity values.
- "step_beg=1.0": the initial step length.
- "step_min=1.0e-3" and "step_max=5.0": the minimum and maximum step lengths.
- "reg_method=1": the type of regularization.
- "reg_par=1.0": the value of regularization parameter.

SUMMARY

A computer program for seismic modeling, migration, and inversion based on the acoustic wave equation was presented with details about the methods used and the program usage instructions. Numerical examples for each type of computation were given to demonstrate its use and performance. Currently, the program simply performs parallel computation using the shot number, and only the finite-difference method is available as the numerical method for solving the wave equation. In the future version, we will use domain decomposition for parallelization and will provide more numerical methods including the finite-element and pseudo-spectral methods.

PML VERSIONS OF THE WAVE EQUATIONS

The PML equation for the constant-density acoustic wave equation is given by

$$\left[\frac{\partial^2 p}{\partial t^2} - v^2\left(\frac{\partial^2 p}{\partial x^2}+\frac{\partial^2 p}{\partial z^2}\right)\right] + \left[(\sigma_x+\sigma_z)\frac{\partial p}{\partial t} + \sigma_x\sigma_z p - v^2\left\{\sigma_z\frac{\partial \psi_x}{\partial x} - \frac{\partial(\sigma_x\psi_x)}{\partial x} + \sigma_x\frac{\partial \psi_z}{\partial z} - \frac{\partial(\sigma_z\psi_z)}{\partial z}\right\}\right] = s(x,z,t) \quad \text{(A-1)}$$

where ψ_x and ψ_z are the auxilliary fields satisfying

$$\frac{\partial \psi_x}{\partial t} = -\sigma_x\psi_x + \frac{\partial p}{\partial x}, \quad \text{(A-2)}$$

$$\frac{\partial \psi_z}{\partial t} = -\sigma_z\psi_z + \frac{\partial p}{\partial z}, \quad \text{(A-3)}$$

and σ_x and σ_z are damping parameters which are non-zero in the PML regions.

The PML equations for the variable-density acoustic wave equation are given by

$$\frac{\partial p}{\partial t} + (\sigma_x+\sigma_z)p + \sigma_x\sigma_z\phi - \kappa\left(\sigma_z\frac{\partial \phi_x}{\partial x} + \frac{\partial v_x}{\partial x} + \sigma_x\frac{\partial \phi_z}{\partial z} + \frac{\partial v_z}{\partial z}\right) = s'(x,z,t) \quad \text{(A-4)}$$

$$\frac{\partial v_x}{\partial t} + \sigma_x v_x = -\frac{1}{\rho}\frac{\partial p}{\partial x}, \quad \text{(A-5)}$$

$$\frac{\partial v_z}{\partial t} + \sigma_z v_z = -\frac{1}{\rho}\frac{\partial p}{\partial z}, \quad \text{(A-6)}$$

where ϕ, ϕ_x, and ϕ_z are the auxilliary fields satisfying

$$\frac{\partial \phi}{\partial t} = p, \quad \text{(A-7)}$$

$$\frac{\partial \phi_x}{\partial t} = v_x, \quad \text{(A-8)}$$

$$\frac{\partial \phi_z}{\partial t} = v_z. \quad \text{(A-9)}$$

The derivation of the PML equations are presented in Boonyasiriwat (2013).

INPUT PARAMETER FILE FOR FULL-WAVEFORM INVERSION

The following input parameters are the content of the input file used in the example shown in the usage section.

```
jobtype=inversion
gridtype=standard
fd_order=4
velfile_in=vel.dat
densityfile=n/a
coordfile=coord.dat
topofile=n/a
nx=501
nz=401
dx=10.0
nt=4001
dt=0.001
freq=10.0
sourcefile=n/a
csg_in_prefix=csg
npml=50
free_surface=1
itermax=20
vmin=1500.0
vmax=4500.0
step_beg=1.0
```

```
step_min=0.001
step_max=5.0
reg_method=1
reg_par=1.0
multisrc_file=nsg1_nss100.dat
nsg=1
nss=100
```

ACKNOWLEDGMENTS

This work was supported by the Thailand Research Fund, the Higher Education, and the Mahidol University under the research grant MRG5480280. We are also grateful for the support by the PTT Exploration and Production, Plc.

REFERENCES

Boonyasiriwat, C., 2013, Perfectly matched layer (PML) for full-waveform modeling of seismic and electromagnetic wave propagation in unbounded domains. Mahidol University Center for Scientific Computing, Midyear Report, 59-63.

Boonyasiriwat, C., G. T. Schuster, P. Valasek, and W. Cao, 2010, Application of multiscale waveform inversion to marine data using a flooding technique and dynamic early-arrival windows: Geophysics, **75**, R129–136.

Boonyasiriwat, C., P. Valasek, W. Cao, G. T. Schuster, and B. Macy, 2009, An efficient multiscale method for time-domain waveform tomography: Geophysics, **74**, WCC59–WCC68.

Bunks, C., F. M. Saleck, S. Zaleski, and G. Chavent, 1995, Multiscale seismic waveform inversion: Geophysics, **60**, 1457–1473.

Krebs, J., J. E. Anderson, D. Hinkley, R. Neelamani, S. Lee, A. Baumstein, and M. Lacasse, 2009, Fast full-wavefield seismic inversion using encoded sources: Geophysics, **74**, WCC177–WCC188.

Robertsson, J., 1996, A numerical free-surface condition for elastic/viscoelastic finite-difference modeling in the presence of topography: Geophysics, **61**, 1921–1934.

Schuster, G. T., X. Wang, Y. Huang, W. Dai, and C. Boonyasiriwat, 2011, Theory of multisource crosstalk reduction by phase-encoded statics: Geophysical Journal International, **184**, 1289–1303.

Sheng, J., A. Leeds, M. Buddensiek, and G. T. Schuster, 2006, Early arrival waveform tomography on near-surface refraction data: Geophysics, **71**, U47–U57.

Sourbier, F., S. Operto, J. Virieux, P. Amestoy, and J. L'Excellent, 2009, FWT2D: A massively parallel program for frequency-domain full-waveform tomography of wide-aperture seismic data-Part 1: Computers and Geosciences, **35**, 487–495.

Tarantola, A., 1984, Inversion of seismic reflection data in the acoustic approximation: Geophysics, **49**, 1259–1266.

Vigh, D. and E. W. Starr, 2008, 3d prestack plane-wave, full-waveform inversion: Geophysics, **73**, VE135–VE144.

Zhang, J. and Z. Yao, 2013, Optimized finite-difference operator for broadband seismic wave modeling: Geophysics, **78**, A13–A18.

JIMMI: Java Interface to MMI

Numchoke Boonyasiriwat and Chaiwoot Boonyasiriwat

ABSTRACT

MMI is an in-house program developed for seismic imaging research. This program has no user interface and can only be executed through command prompt. The program also required a parameter file as an input. The problem is that some students are not familiar with a command prompt and they have to manually create a parameter file which can cause the program error if a parameter file is incorrect. In this project, we develop a graphical user interface (GUI) for MMI. The program has input fields for receiving parameter values specified by the user. A parameter file will be automatically created by a program which can prevent a human error. In addition, the user does not need to run MMI through a command prompt anymore. They just click a button on this GUI program and MMI will be executed. We hope that this program will help the students to do their research more efficiently and also be a valuable research tool.

INTRODUCTION

Java is a computer programming language that is concurrent, class-based, object-oriented, and specifically designed to have as few implementation dependencies as possible. The program code that runs on one platform does not need to be recompiled to run on another platform. Java applications are typically compiled to bytecode (class file) that can run on any Java virtual machine (JVM) regardless of computer architecture. Java was originally developed by James Gosling at Sun Microsystems and released in 1995 as a core component of Sun Microsystems' Java platform. The language derives much of its syntax from C and C++, but it has fewer low-level facilities than either of them.

'Java Interface to MMI (JIMMI)' is a Java based application which used as an interface to MMI application. JIMMI is designed to recieve the input parameters for running the modeling, migration and inversion jobs. The job is mainly processed through MMI application.

GETTING STARTED

This section provides a general walkthrough of the system from initiation through exit.

Logging On

The application can be accessed by opening a command prompt and typing command 'jimmi.sh' (Figure 1).

Fig/logon.png

Figure 1: Running JIMMI from the terminal

System Menu

The application is consisted of 3 main menus as follows (Figure 2):

- Job menu: This menu is used for opening a new job (modeling, migration, inversion) window and import the parameter file.
- Image menu: This menu is used for opening the output image file.
- Setting menu: This menu is used for setting program configuration.

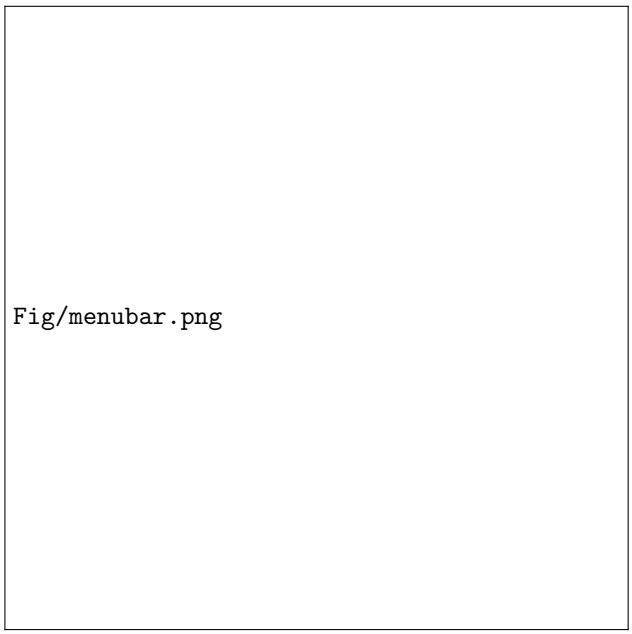

Figure 2: System menu

Exit System

The application can be closed by selecting exit menu or clicking the symbol 'x' at the top left corner of main window (Figure 3).

USING THE SYSTEM

This section provides a detailed description of system functions.

New Job Menu: Modeling

- The user can run modeling by selecting 'Modeling' under 'New Job' menu (Figure 4).
- The 'New Modeling Job' window is consisted of 8 parts as follows (Figure 5):
  - Modeling Type: The user can select the modeling type in this part.
  - Finite Difference Parameters: This part requires the user to fill-in the finite difference parameters.
  - Velocity Density models: This part requires the user to setup the velocity and/or density models.

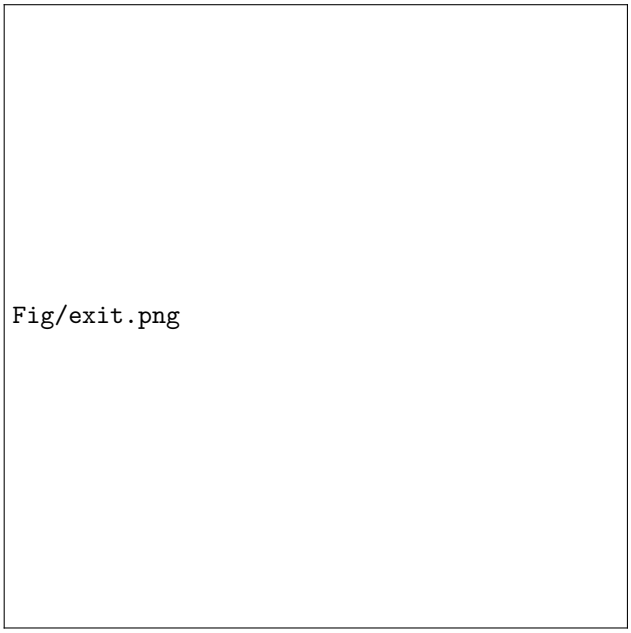

Figure 3: Exit menu

  - Topography: The user can add the topography file in this part (optional).
  - Acquisition Information: This part requires the user to select the coordinate file.
  - Source Information: This part requires the user to setup the source information.
  - Program Execution Parameters: The user can select whether to run the program in serial mode or parallel mode.
  - Data Directory: The user can select the location of output file from this part.
- After completion of all parts, the user can save all information into file by selecting 'Save Parameter to File' button and then click on 'Run MMI' button to execute the program. If the user clicks the 'Cancel' button, this window will be closed and the job will not be executed. The 'Load Parameter File' button is used for importing the parameter file into the program. This step is also applied to migration and inversion execution.
- The 'New Modeling Job' window will be closed after finish running and the job details will be displayed in the 'Submitted Job Log' table at main window (Figure 6). From this window, the user can view the output file by clicking the 'Open' button and selecting the file to be viewed. The output image will be displayed as shown in Figure 7. This step is also applied to migration and inversion execution.

New Job Menu: Migration

- The user can run migration by selecting 'Migration' under 'New Job' menu (Figure 8).

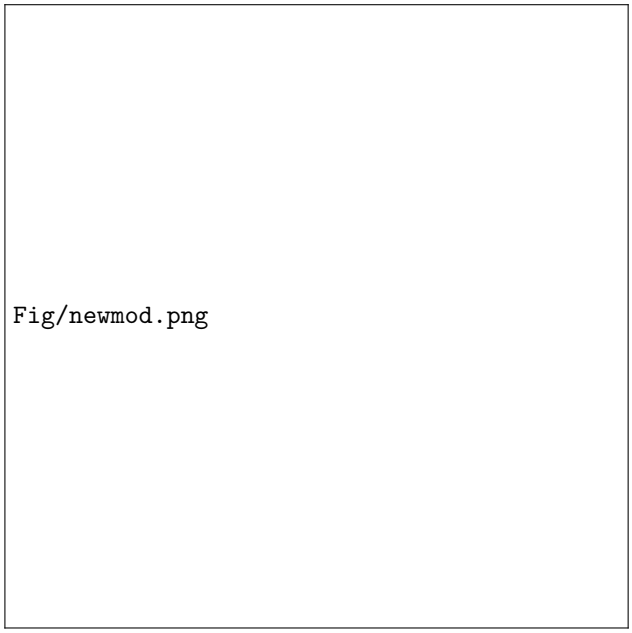

Figure 4: Modeling menu

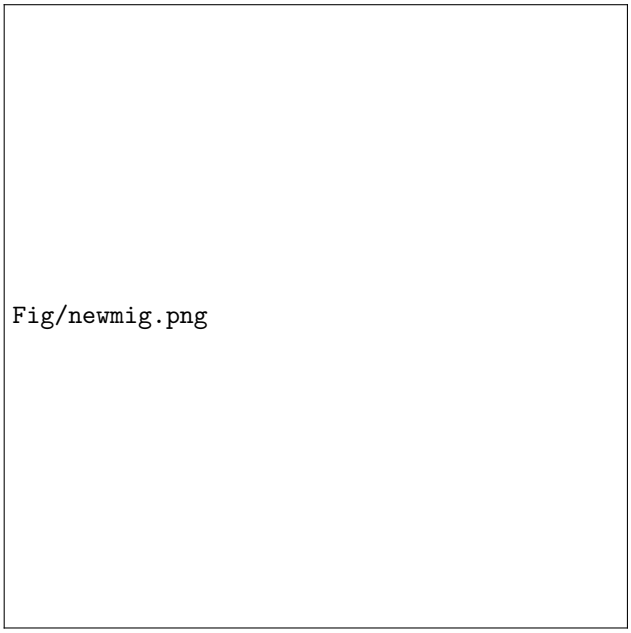

Figure 8: Migration menu

- The 'New Migration Job' window is consisted of 8 parts as follows (Figure 9):
  - Migration Type: The user can select the migration type in this part.
  - Finite Difference Parameters: This part requires the user to fill-in the finite difference parameters.
  - Velocity Density models: This part requires the user to setup the velocity and/or density models.
  - Topography: The user can add the topography file in this part (optional).
  - Acquisition Information: This part requires the user to select the coordinate file.
  - Source Information: This part requires the user to setup the source information.
  - Program Execution Parameters: The user can select whether to run the program in serial mode or parallel mode.
  - Data Directory: This part requires the user to select the input file directory. The user can also select the location of output file from this part.

New Job Menu: Inversion

- The user can run inversion by selecting 'Inversion' under 'New Job' menu (Figure 10).
- The 'New Inversion Job' window is consisted of 9 parts as follows (Figure 11):
  - Inversion Type: The user can select the migration type in this part.
  - Inversion Parameters: This part requires the user to fill-in the inversion parameters.
  - Finite Difference Parameters: This part requires the user to fill-in the finite difference parameters.
  - Velocity Density models: This part requires the user to setup the velocity and/or density models.
  - Topography: The user can add the topography file in this part (optional).
  - Acquisition Information: This part requires the user to select the coordinate file.
  - Source Information: This part requires the user to setup the source information.
  - Program Execution Parameters: The user can select whether to run the program in serial mode or parallel mode.
  - Data Directory: This part requires the user to select the input file directory. The user can also select the location of output file from this part.

Open Job Menu

- The user can import a parameter file which is in XML format into the application via the 'Open Job' menu (Figure 12).

Open Image Menu

- The user can open the image file which is in SU format via the 'Open Image' menu (Figure 13).

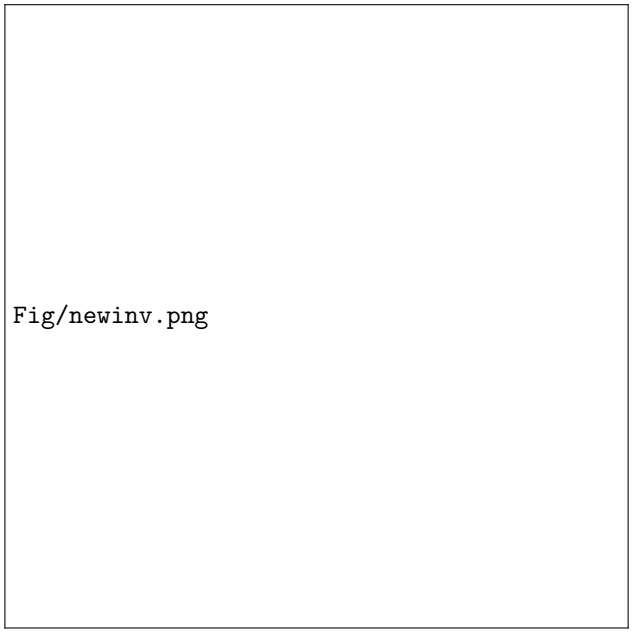

Figure 10: Inversion menu

Setting Menu

- The user can reset the path of MMI application via the 'Set MMI Full Path' menu (Figure 14).
- The user can reset the path of MPIEXEC application via the 'Set MPIEXEC Full Path' menu (Figure 14).

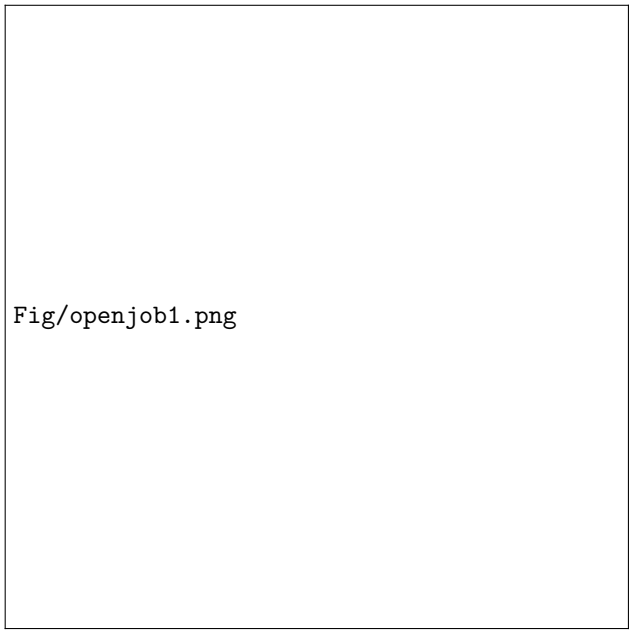

Figure 12: Open Job menu

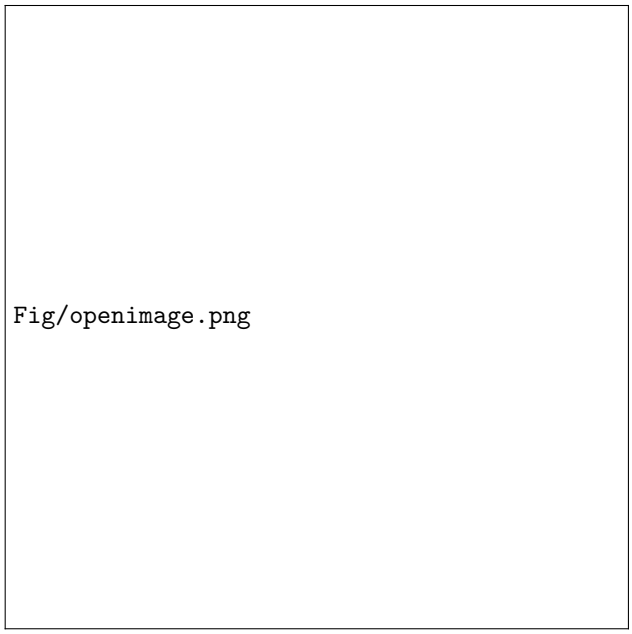

Figure 13: Open Image menu

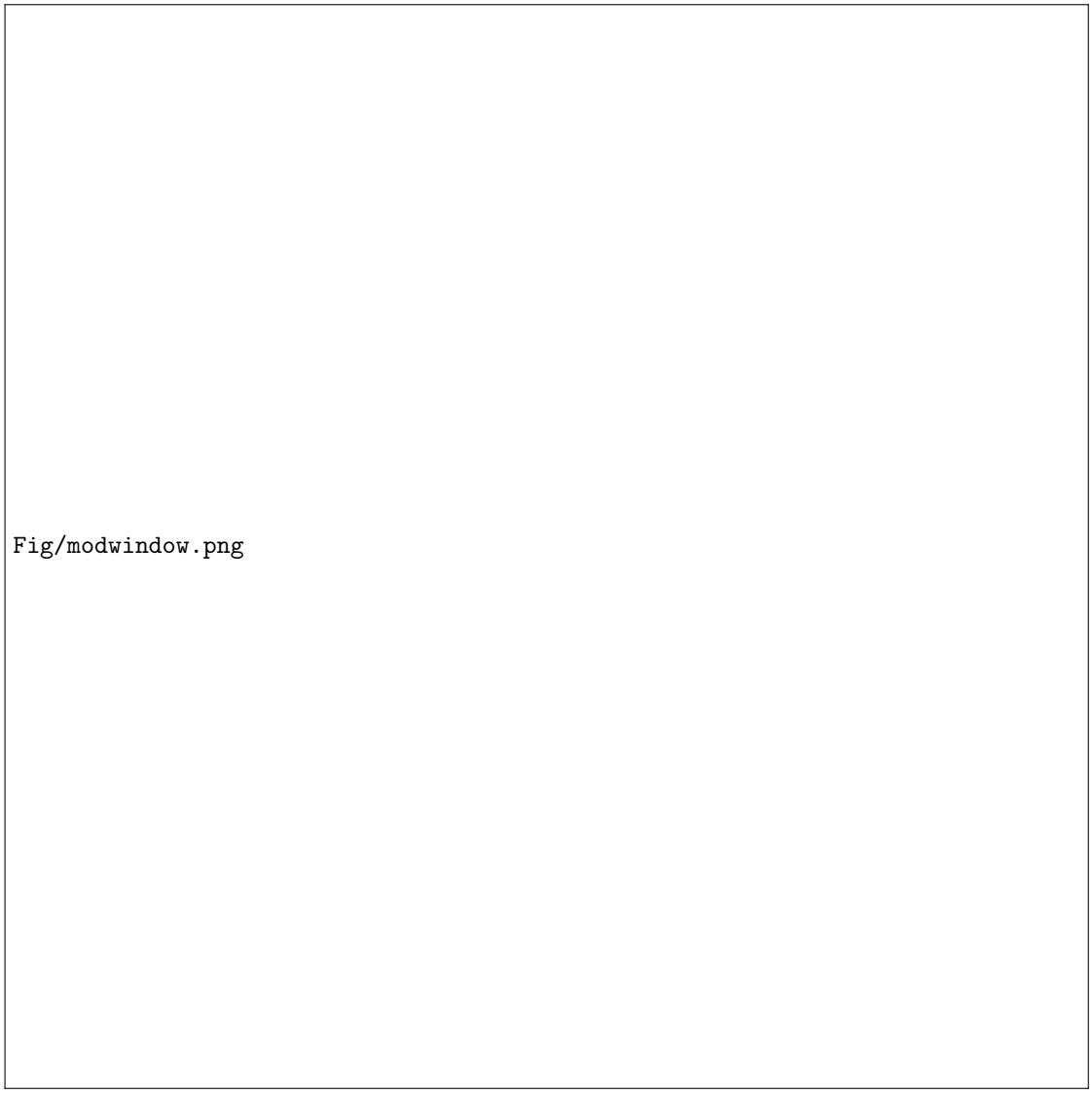

Figure 5: New Modeling Job window

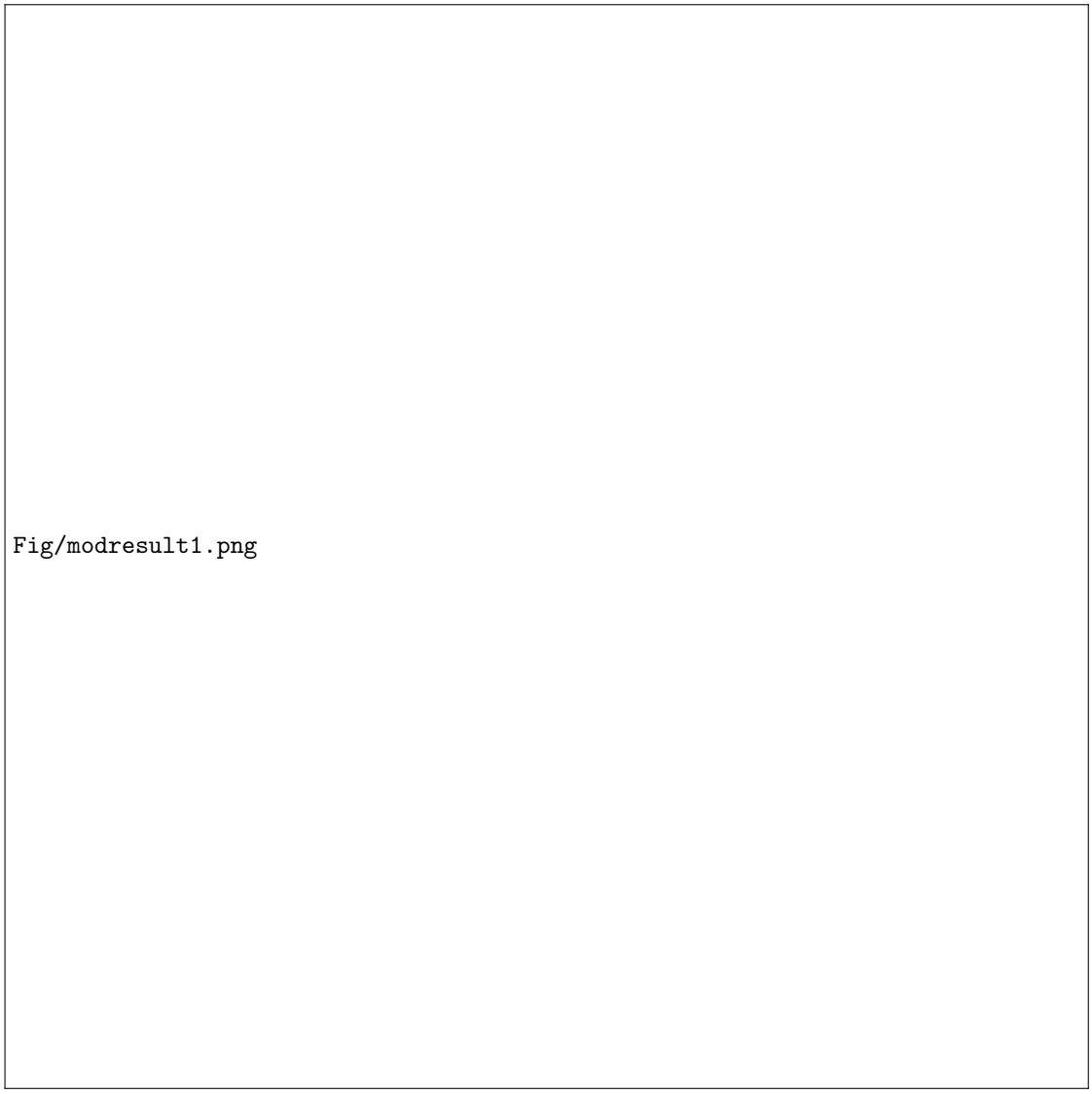

Figure 6: Submitted Job Log table

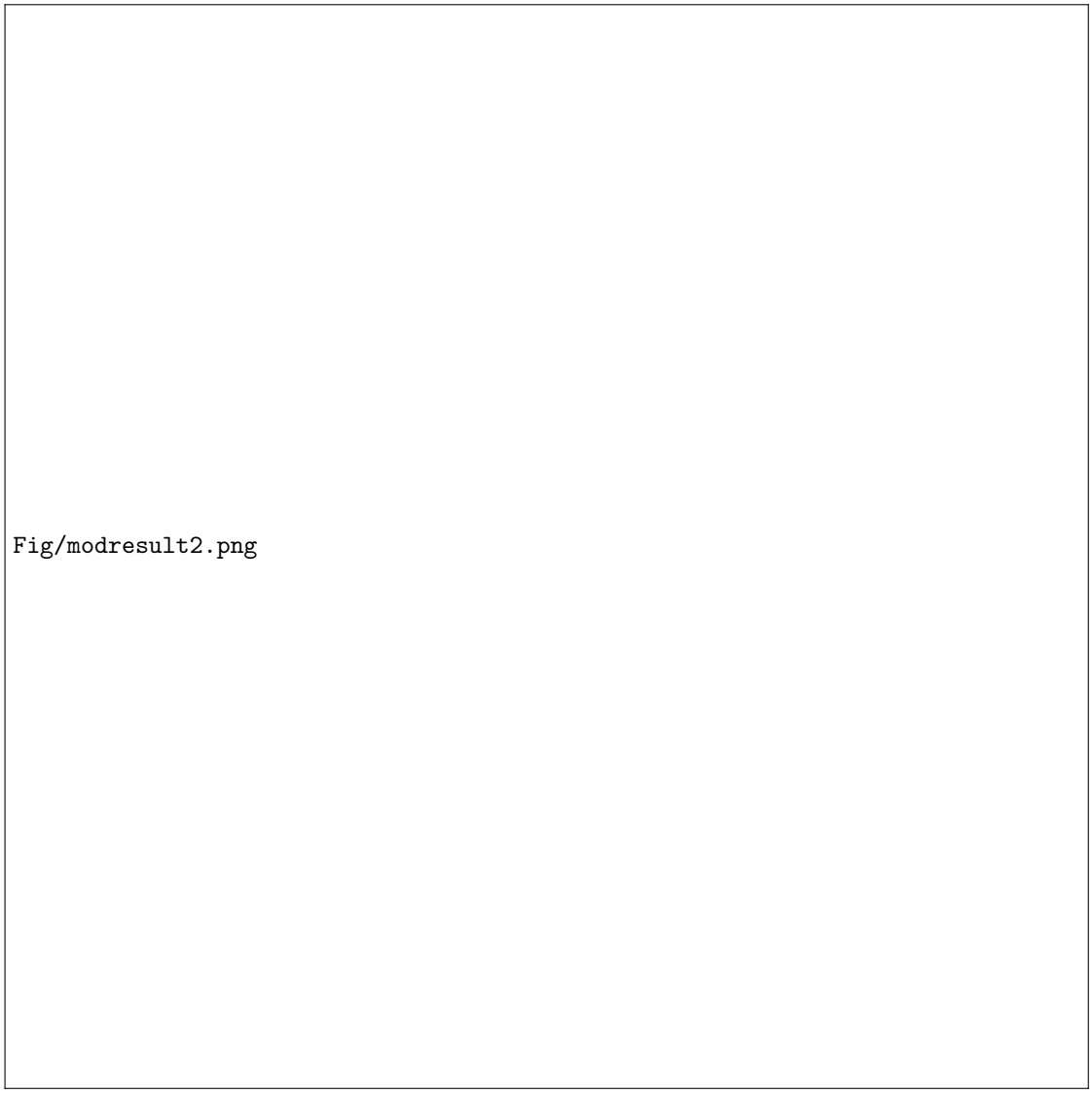

Figure 7: Output image

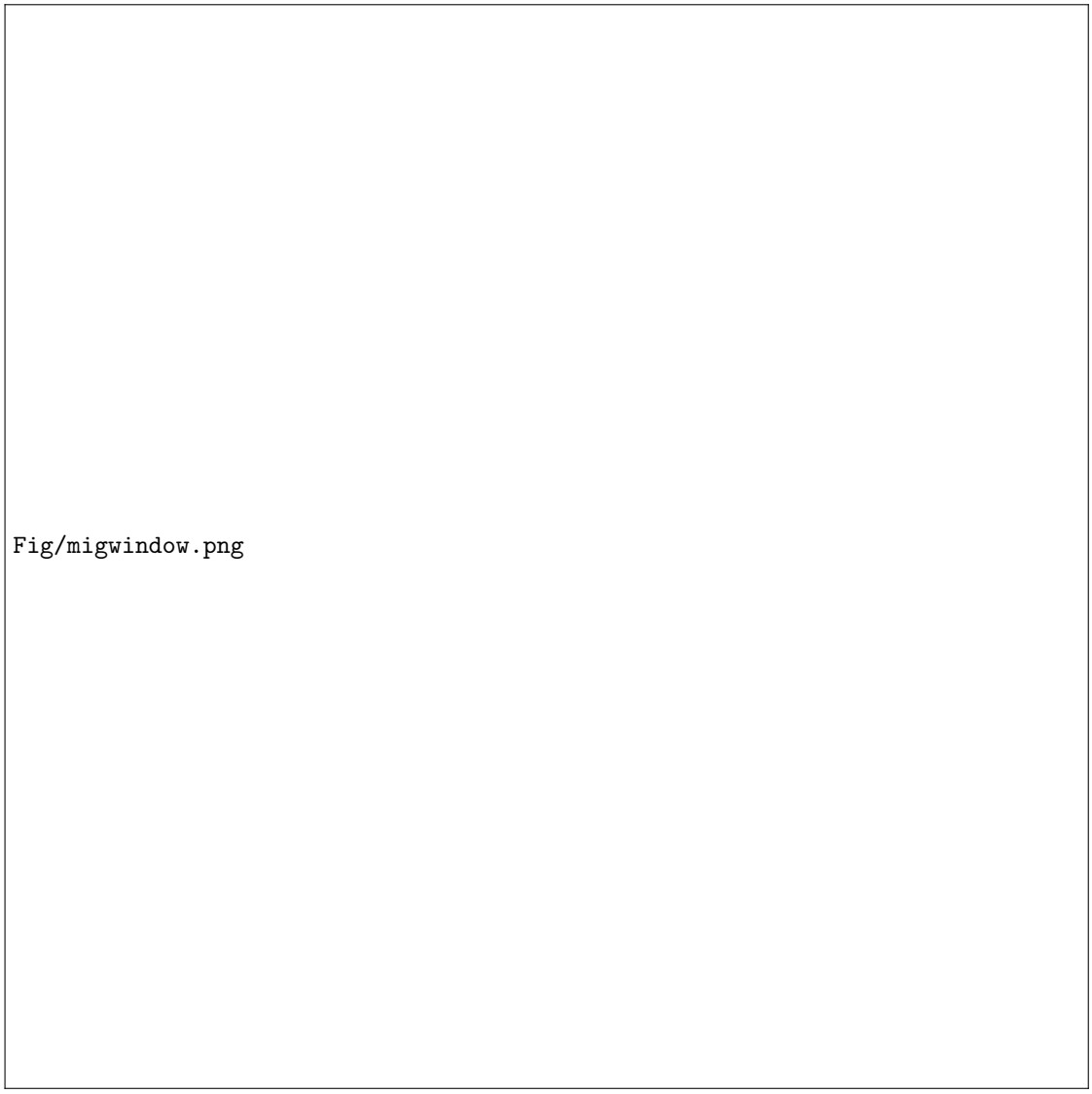

Figure 9: New Migration Job window

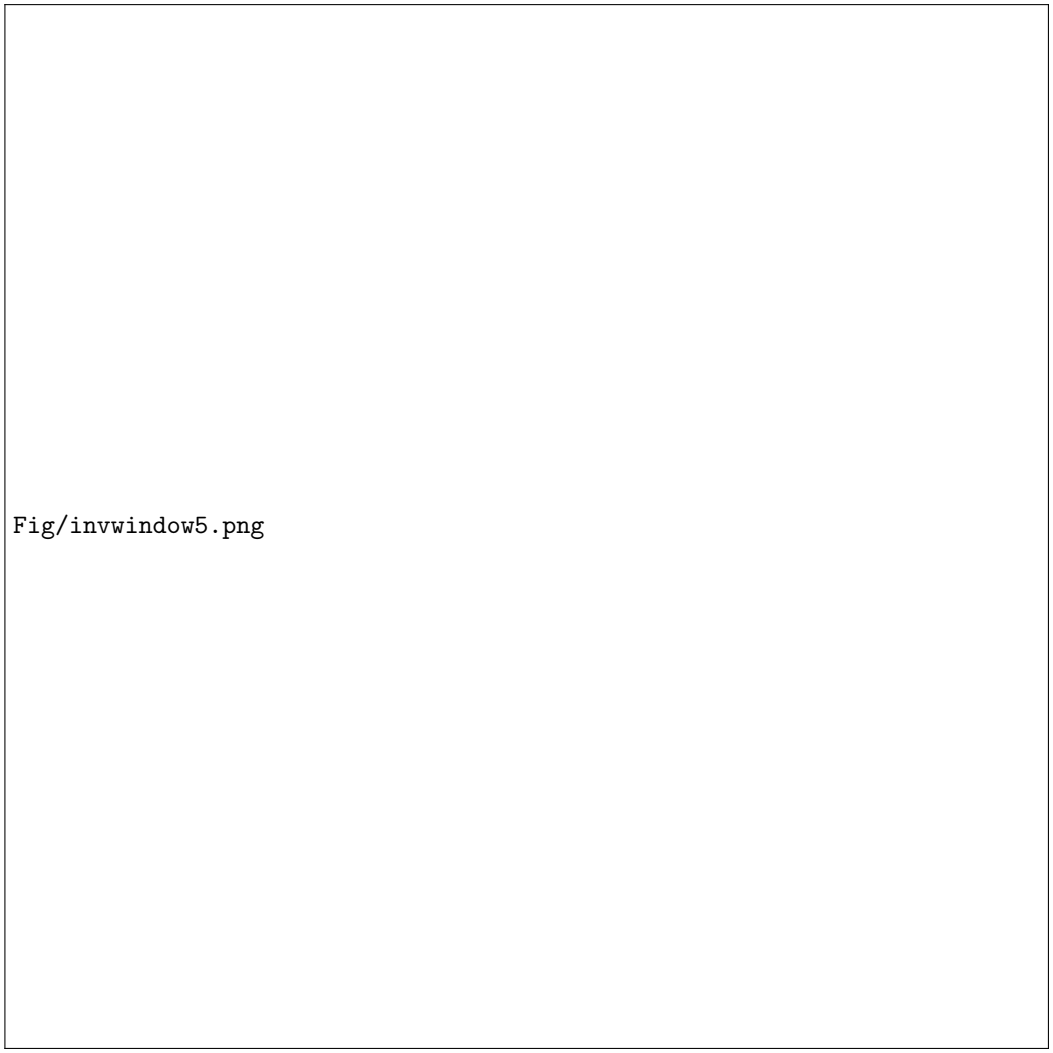

Figure 11: New Inversion Job window